

**RUMBLE STRIP DESIGN EVALUATION
BASED ON EXTERIOR NOISE USING
FINITE ELEMENT ANALYSIS**

Final Report

PROJECT OSU31167



Oregon Department of Transportation

**RUMBLE STRIP DESIGN EVALUATION BASED ON
EXTERIOR NOISE USING FINITE ELEMENT ANALYSIS**

Final Report

PROJECT OSU31167

by
Paris Kalathas
Dr. Christopher Parrish
Dr. Yue Zhang
Oregon State University

for

Oregon Department of Transportation
Research Section
555 13th Street NE, Suite 1
Salem OR 97301

and

April 2019

1. Report No. OR-RD-19-10	2. Government Accession No.	3. Recipient's Catalog No.	
4. Title and Subtitle RUMBLE STRIP DESIGN EVALUATION BASED ON EXTERIOR NOISE USING FINITE ELEMENT ANALYSIS		5. Report Date -April 2019	6. Performing Organization Code
7. Author(s) Paris Kalathas, Dr. Christopher Parrish, Dr. Yue Zhang		8. Performing Organization Report No.	
9. Performing Organization Name and Address Oregon Department of Transportation Research Section 555 13 th Street NE, Suite 1 Salem, OR 97301		10. Work Unit No. (TRAIS)	11. Contract or Grant No.
12. Sponsoring Agency Name and Address Oregon Dept. of Transportation Research Section 555 13 th Street NE, Suite 1 Salem, OR 97301		13. Type of Report and Period Covered Final Report	
15. Supplementary Notes Technical Advisory Committee: ODOT: Kira Glover-Cutter (Coordinator, Chair), Mike Kimlinger (Project Champion), Kevin Haas, Eric Leaming, Joel McCarroll, Carole Newvine, Katherine Burns		14. Sponsoring Agency Code	
16. Abstract Using an alternative, physical-based approach for experimentation with rumble strips, twenty new rumble strip patterns were developed and investigated. The specific aim of this research was to identify modeled rumble strip designs that provide maximum safety by capturing driver attention through tactile and audible signals while also maintaining low noise emissions to the surrounding area. Specifically, this study used static state finite element analysis (FEA) to simulate the tire rolling on the rumble strip designs. Both the dBA level and the 1/3 octave analysis frequency spectra were extracted from each design simulation. The results from this modeling analysis together with published field measurements revealed six promising designs for future in-depth modeling and potential field analysis, including three new sinusoidal and three newly developed sawtooth designs. While different variations of the sinusoidal rumble strip design have been tested and implemented by other DOTs, the modeling results from this work suggest that this new sawtooth rumble strip design reduces exterior noise levels even more than published sinusoidal patterns.			
17. Key Words Rumble strips, sound level, noise contours, finite element analysis		18. Distribution Statement Copies available from NTIS, and online at www.oregon.gov/ODOT/TD/TP_RES/	
19. Security Classification (of this report) Unclassified	20. Security Classification (of this page) Unclassified	21. No. of Pages 54	22. Price

SI* (MODERN METRIC) CONVERSION FACTORS

APPROXIMATE CONVERSIONS TO SI UNITS					APPROXIMATE CONVERSIONS FROM SI UNITS				
Symbol	When You Know	Multiply By	To Find	Symbol	Symbol	When You Know	Multiply By	To Find	Symbol
<u>LENGTH</u>					<u>LENGTH</u>				
in	inches	25.4	millimeters	mm	mm	millimeters	0.039	inches	in
ft	feet	0.305	meters	m	m	meters	3.28	feet	ft
yd	yards	0.914	meters	m	m	meters	1.09	yards	yd
mi	miles	1.61	kilometers	km	km	kilometers	0.621	miles	mi
<u>AREA</u>					<u>AREA</u>				
in ²	square inches	645.2	millimeters squared	mm ²	mm ²	millimeters squared	0.0016	square inches	in ²
ft ²	square feet	0.093	meters squared	m ²	m ²	meters squared	10.764	square feet	ft ²
yd ²	square yards	0.836	meters squared	m ²	m ²	meters squared	1.196	square yards	yd ²
ac	acres	0.405	hectares	ha	ha	hectares	2.47	acres	ac
mi ²	square miles	2.59	kilometers squared	km ²	km ²	kilometers squared	0.386	square miles	mi ²
<u>VOLUME</u>					<u>VOLUME</u>				
fl oz	fluid ounces	29.57	milliliters	ml	ml	milliliters	0.034	fluid ounces	fl oz
gal	gallons	3.785	liters	L	L	liters	0.264	gallons	gal
ft ³	cubic feet	0.028	meters cubed	m ³	m ³	meters cubed	35.315	cubic feet	ft ³
yd ³	cubic yards	0.765	meters cubed	m ³	m ³	meters cubed	1.308	cubic yards	yd ³
*NOTE: Volumes greater than 1000 L shall be shown in m ³ .									
<u>MASS</u>					<u>MASS</u>				
oz	ounces	28.35	grams	g	g	grams	0.035	ounces	oz
lb	pounds	0.454	kilograms	kg	kg	kilograms	2.205	pounds	lb
T	short tons (2000 lb)	0.907	megagrams	Mg	Mg	megagrams	1.102	short tons (2000 lb)	T
<u>TEMPERATURE (exact)</u>					<u>TEMPERATURE (exact)</u>				
°F	Fahrenheit	(F-32)/1.8	Celsius	°C	°C	Celsius	1.8C+32	Fahrenheit	°F

*SI is the symbol for the International System of Measurement

ACKNOWLEDGEMENTS

We would like to thank Dr. Kira Glover-Cutter of the Oregon Department of Transportation for her guidance, generous help and support. Dr. Glover-Cutter made multiple trips to Oregon State University to meet with the project team and provided invaluable input on all aspects of the project, from the literature review through the final report preparation. We also thank the members of the TAC, Kevin Hass, Katherine Burns, Eric Leaming, Joel McCarroll, Carole Newvine, and Mike Kimlinger, for their feedback throughout the project and ODOT Chief Engineer, Bob Pappé, for supporting this work. We also thank Oregon State University graduate student, Laura Barreiro Fernandez, for her work on the sound propagation modeling portion of the study.

DISCLAIMER

This document is disseminated under the sponsorship of the Oregon Department of Transportation and the United States Department of Transportation in the interest of information exchange. The State of Oregon and the United States Government assume no liability of its contents or use thereof.

The contents of this report reflect the view of the authors who are solely responsible for the facts and accuracy of the material presented. The contents do not necessarily reflect the official views of the Oregon Department of Transportation or the United States Department of Transportation.

The State of Oregon and the United States Government do not endorse products of manufacturers. Trademarks or manufacturers' names appear herein only because they are considered essential to the object of this document.

This report does not constitute a standard, specification, or regulation.

TABLE OF CONTENTS

EXECUTIVE SUMMARY	IX
1.0 INTRODUCTION.....	1
2.0 BACKGROUND	3
2.1 RUMBLE STRIPS	3
2.2 dB _{SPL} / NOISE LEVELS	4
2.3 A-WEIGHT FILTER.....	4
2.4 FREQUENCY SPECTRUM - 1/3 OCTAVE ANALYSIS.....	5
3.0 LITERATURE REVIEW	7
3.1 NATIONAL HIGHWAY COOPERATIVE RESEARCH PROJECT (NHCRP) REPORT 641, “GUIDANCE FOR THE DESIGN AND APPLICATION OF SHOULDER AND CENTERLINE RUMBLE STRIPS”, 2009	7
3.2 SEXTON T.V., “EVALUATION OF CURRENT CENTERLINE RUMBLE STRIP DESIGNS TO REDUCE ROADSIDE NOISE AND PROMOTE SAFETY”, WSDOT, 2014	7
3.3 TERHAAR E., “RUMBLE STRIP NOISE EVALUATION”, MNDOT, 2015	8
3.4 WANG BINXING ET AL., “ACOUSTIC MODELLING AND ANALYSIS OF VEHICLE INTERIOR NOISE BASED ON NUMERICAL CALCULATION”, 2010.....	10
3.5 KIM ET AL., "DESIGN AND EVALUATION OF MODIFIED CENTERLINE RUMBLE STRIPS", NDOR, 2017	10
4.0 THE FEA APPROACH	13
4.1 RUMBLE STRIP PROFILE DEVELOPMENT	13
4.2 CALCULATION PROCEDURE	14
5.0 RESULTS	15
5.1 COMPARISON AMONG THE 20 DESIGNS	15
5.2 SIX SELECTED RUMBLE STRIP DESIGNS.....	16
5.3 NOISE CONTOUR MODELING FOR VISUAL ANALYSIS OF RUMBLE STRIP DESIGN IMPACTS 18	18
6.0 CONCLUSION	23
7.0 FUTURE WORK.....	25
8.0 REFERENCES.....	27
APPENDIX A: 1/3 OCTAVE ANALYSIS FREQUENCY SPECTRA FOR THE TWENTY SIMULATED RUMBLE STRIP DESIGNS	A-1

LIST OF TABLES

Table 5.11: Input to SPreAD-GIS Model Runs.....	21
---	----

LIST OF FIGURES

Figure 2.1: a) Current rumble strip designs. b) Road pavement with shoulder, center-line and transverse rumble strips installed. [From Donovan and Rymer, 2015].	3
Figure 2.2: Common noise sources. Sinusoidal and Cylindrical rumble strip noise output is noted with stars. [From Personal Music Players and Hearing (n.d), 2017].	4
Figure 2.3: Equal-loudness contours (red) (from ISO 226:2003 revision) and Fletcher-Munson curves (blue). [From Hobbs, 2018].	5
Figure 2.4: 1/3 octave analysis center frequencies. [From Octave Band Filters (n.d.), 2017].	6
Figure 3.1: Exterior noise measurements from different rumble strips on different road sites. [From Sexton T.V., 2014].	8
Figure 3.2: Exterior noise measurements for California (sinusoidal), Pennsylvania (sinusoidal) and Minnesota (cylindrical) designs. [From Terhaar and Braslau, 2015].	9
Figure 3.3: Interior noise measurements for California (sinusoidal), Pennsylvania (sinusoidal) and Minnesota (cylindrical) designs. [From Terhaar and Braslau, 2015].	9
Figure 3.4: Before and after optimization frequency levels. [From Wang Binxing et al. 2010].	10
Figure 3.5: 2D modeling and visualization of the stress forces on four rumble strip designs. [From Kim et al., 2017].	11
Figure 4.1: The three main rumble strip profile categories	13
Figure 4.2: Flowchart of computation framework (left), 3D modeling of the tire and road (right).	14
Figure 5.1: dBA values for each design category RS, SS and ST. Top row is for 0.5" depth and bottom is for 0.625" depth. The middle number is wavelength.	15
Figure 5.2: 1/3 octave analysis frequency spectra for all the simulated designs. Please also refer to Appendix A for individual analysis.	16
Figure 5.3: dBA values for all the six suggested designs	17
Figure 5.4: 1/3 octave frequency spectra for flat road and the sinusoidal designs	17
Figure 5.5: 1/3 octave frequency spectra for flat road and the sawtooth designs	18
Figure 5.6: Analysis of La Grande project site in Google Earth.	19
Figure 5.7: DOGAMI lidar point cloud data for La Grande project site viewed in QCoherent's LP360 software.	20
Figure 5.8: Noise contour maps based on mean sound levels for three rumble strip design categories (rectified sinusoidal - RS, sinusoidal - SS, and sawtooth - ST) with 0.5" depth for La Grande project site.	21
Figure 5.9: Noise contour maps based on mean sound levels for three rumble strip design categories (rectified sinusoidal - RS, sinusoidal - SS, and sawtooth - ST) with 0.625" depth for La Grande project site.	22

EXECUTIVE SUMMARY

This study presents six new rumble strip designs for future field-based examination. These designs are derived from computer modeling and finite element analysis calculations. The goal of this study was to design new rumble strip patterns that maintain the safety that rumble strips offer, while also minimizing noise radiation to the surrounding environment through fine tuning current designs or creating new designs.

The development of optimal designs without computer modelling would have been extremely challenging due to the limited availability of studies with exterior noise measurements. From what is currently available in the literature, only four publications include exterior noise measurements with frequency spectra. Furthermore, suggested formulas and noise prediction models associated with rumble strip analysis focus on the rumble strip interior feedback, denoted as interior noise and not on the noise projected to the external environment (Torbic et al., 2009).

Twenty new designs were created based on general guidelines from the literature and from theoretical calculations on the parameters of each design. The designs are separated in three main groups based on shape: “Rectified Sinusoidal (RS)”, “Sinusoidal (SS)” and “Sawtooth (ST).” The tire speed for the simulations was 37.3 mph (60 km/h) and the tire dimension used was 175SR14.

The results include the dBA level for all designs along with associated 1/3 octave analysis frequency spectra from 20 – 500 Hz. This low frequency range was selected based on the literature, where is mentioned that lower frequencies travel further and create most of the perceived disturbance (Sexton, 2014). The measurement point for analysis was inside the tire; thus, more reduction on the dBA level is expected for some frequencies as the noise distributes.

The general observation is that deeper designs with shorter wavelengths create higher noise levels with complex frequency spectra. The results from the rectified sinusoidal and sinusoidal designs reveal similar frequency excitations, which are focused mainly at the 79 Hz. Rectified sinusoidal designs have some additional higher harmonic peaks at 315 and 400 Hz. Compared to the other two categories, sawtooth designs showed reduced noise emission levels and smoother frequency spectrum, with a small excitation peak at 125 Hz, and significantly reduced peak excitation at the lower 79 Hz.

1.0 INTRODUCTION

This study is the first part of a series of potential studies that analyze milled shoulder rumble strips (SRS) using computer modeling and simulation. Multiple studies have concluded that shoulder rumble strips are an efficient lane departure counter-measure, but when they are installed near residential areas, complaints are often filed to Departments of Transportation (DOTs) from residents regarding noise (CTC and Associates LLC, 2012). To address this problem, DOTs have been investigating ways to modify rumble strip dimensions or create different rumble strip designs. However, to construct and test different designs requires various equipment, which can be costly. Therefore, Oregon DOT is exploring alternative methods that may provide an initial understanding and classification for the designs under investigation before proceeding to installation and field measurements. The primary objective of this study is to recommend 6 new rumble strip designs for construction and further examination. This includes provision of dimensions, wavelength, width and depth as well as theoretical calculation of noise levels (dBA), exterior sound level difference (SLD) from a reference value (flat road), and the exterior low frequency range of the associated frequency spectrum.

2.0 BACKGROUND

This section introduces technical terms that will be used throughout the report and provides an overview of rumble strip utility.

2.1 RUMBLE STRIPS

Rumble strips are road devices that can be installed on the pavement shoulder, centerline, and in a transverse direction to a traveling vehicle. Rumble strips produce audible and tactile signals to alert drivers of lane departures and act as a speed mitigation measure (Fig. 2.1b, Hardwood, 1993).

Currently there are two designs for milled SRS, the cylindrical and the sinusoidal (Fig. 2.1a, Smadi and Hawkins, 2016). The cylindrical design functionality is based on the tire falling into the grooves. The fall creates pressure to the tire and to the air in the groove's cavity between the tire and the pavement, resulting in noise and vibrations. The sinusoidal design functionality is based on the wavy movement of the tire on the rumble strips. Cavities may appear on the later as well if the wavelength of the rumble strip is smaller than the contact patch of the tire with the road.

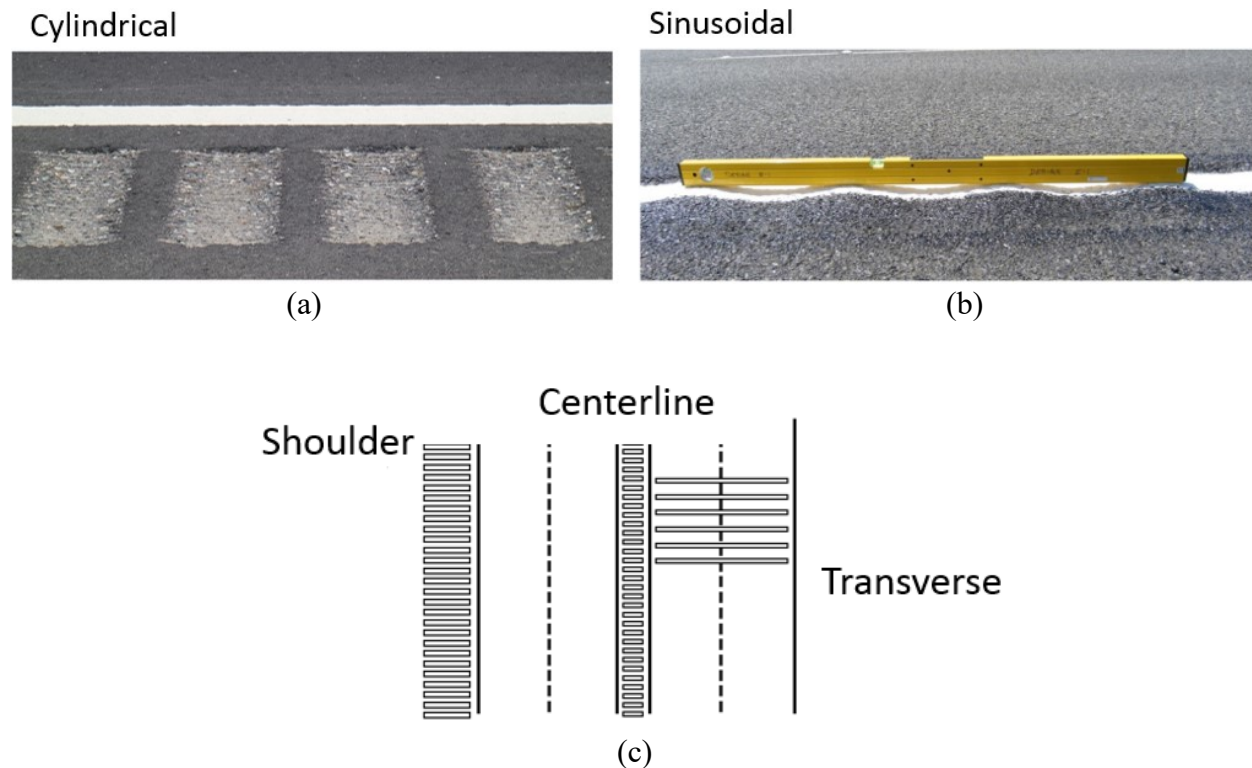


Figure 2.1: a) Current rumble strip designs. b) Road pavement with shoulder, center-line and transverse rumble strips installed. [From Donovan and Rymer, 2015].

2.2 dB_{SPL} / NOISE LEVELS

dB_{spl} (Sound Pressure Level) is the unit for measuring sound or acoustic pressure. It is a logarithmic ratio of the existing sound pressure level with respect to a reference sound pressure level, which is the acoustic threshold of the human hearing. The reference sound pressure level is equal to $2 \times 10^5 \text{ Pa}$ and the dB_{spl} value is given by the equation (Personal Music Players & Hearing, 2017):

$$dB_{spl} = 10 \log \frac{p^2}{p_{ref}^2}, \tag{2-1}$$

Figure 2.2 shows some common noise levels, along with the levels from the current sinusoidal and cylindrical designs.

Source / observing situation	Typical sound pressure level (db SPL)
Hearing threshold	0 dB
Leaves fluttering	20 dB
Whisper in an ear	30 dB
Normal speech conversation for a participant	60 dB
Cars/vehicles for a close observer	60-100 dB ★ Sinusoidal ★ Cylindrical
Airplane taking-off for a close observer	120 dB
Pain threshold	120-140 dB

Figure 2.2: Common noise sources. Sinusoidal and Cylindrical rumble strip noise output is noted with stars. [From Personal Music Players and Hearing (n.d), 2017].

2.3 A-WEIGHT FILTER

Sound is composed of frequencies, and the human ear detects frequencies that are in the range of 20-20000 Hz. However, the ear does not perceive those frequencies in the same manner; instead, human hearing is sensitive to frequencies in the high-mid range from 1000-5000 Hz but insensitive to frequencies in the lower and higher range. Additionally, the sensitivity of the human ear depends on the overall sound level, which is measured at the frequency of 1000Hz. Figure 2.3 presents the equal-loudness curves, which show the dB_{spl} levels required for each frequency to be perceived at the sound level (phon) denoted by the curve.

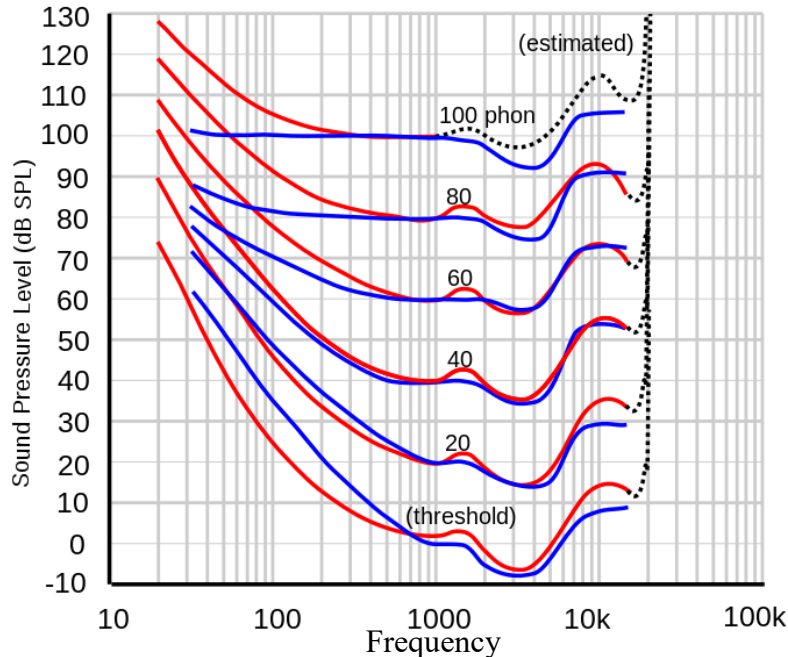


Figure 2.3: Equal-loudness contours (red) (from ISO 226:2003 revision) and Fletcher-Munson curves (blue). [From Hobbs, 2018].

For measuring generated sounds in the same way that the human ear would receive them, the International Telecommunications Union standard ITU-R 468 suggests using the A-weight filter as a standardized conversion for sound measurements (Wikipedia contributors, 2018). The A-weight filter adjusts the level of each frequency to simulate human hearing at the 40 dB_{spl} equal-loudness contour. From this adjustment, the resulting dB values are denoted as dBA values.

2.4 FREQUENCY SPECTRUM - 1/3 OCTAVE ANALYSIS

Since sounds are composed of frequencies that have different sound levels, overall dB_{spl} or dBA values reveal very little information about the impact of that sound to the environment. The human ear receives each frequency differently and each frequency gets absorbed differently through air and objects. This results in lower frequencies traveling further than higher frequencies which are more easily absorbed (Engineering Acoustics/Outdoor Sound Propagation, 2017). In order to examine the frequency content of a sound, measuring equipment visualizes the sound at 1/3 octave analysis resolution. Figure 2.4 demonstrates a typical 1/3 octave representation of a sound. Note the center frequencies of each frequency band and how from this visualization, engineers can identify which frequency bands contribute to the overall level of the sound under investigation.

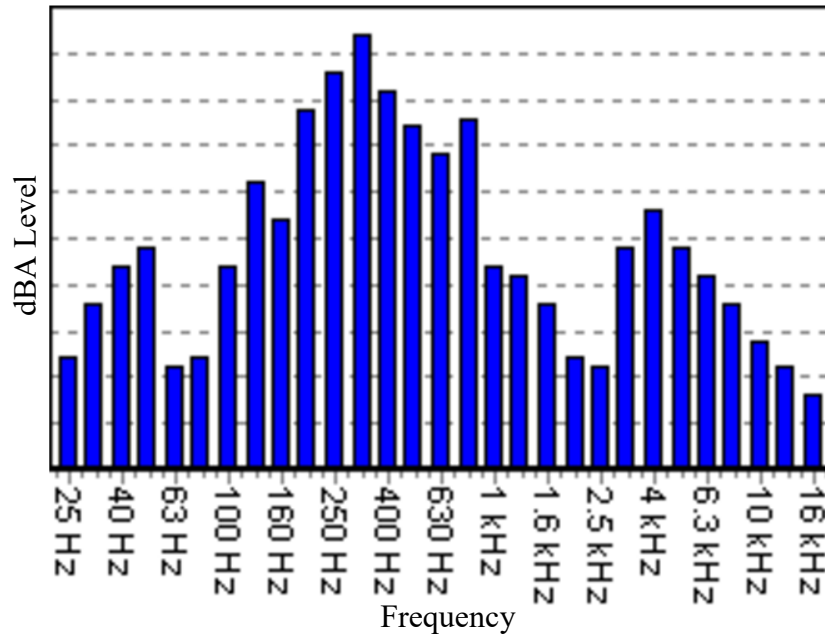


Figure 2.4: 1/3 octave analysis center frequencies. [From Octave Band Filters (n.d.), 2017].

3.0 LITERATURE REVIEW

For this project an extensive review of publications was performed, including technical reports, papers, national reports, master's theses, PhD theses and more. The review was done in order to become familiar with what had been already implemented, what is recommended, and what the limitations are regarding rumble strip designs, testing methods, noise and vibration measurement procedures and standards. In this section, important publications and their outcomes are presented.

3.1 TORBIC D.J., NATIONAL HIGHWAY COOPERATIVE RESEARCH PROJECT (NHCRP) REPORT 641, “GUIDANCE FOR THE DESIGN AND APPLICATION OF SHOULDER AND CENTERLINE RUMBLE STRIPS”, 2009

This is the most current study on rumble strips that includes rumble strip dimension recommendations. The report suggests that wider and deeper rumble strips are more efficient for truck vehicles. It also presents formulas for interior sound level difference (SLD) calculation based on rumble strip dimension, type, position, and vehicle speed, angle of departure, pavement condition, and pavement type. Unfortunately, these formulas are applicable only for cylindrical designs. The threshold ranges for the interior SLD are given for rural roads to be 6 – 12 dBA and for freeways to be 10 – 15 dBA, but the report does not suggest any threshold ranges for vibration levels.

3.2 SEXTON T.V., “EVALUATION OF CURRENT CENTERLINE RUMBLE STRIP DESIGNS TO REDUCE ROADSIDE NOISE AND PROMOTE SAFETY”, WSDOT, 2014

This report presents exterior noise measurements from different rumble strip designs and road types (summarized in Fig. 3.1). One can observe from the measurements provided that modeling exterior noise from this empirical data for new rumble strip designs would be challenging, given that rumble strips with similar dimensions can produce different sound levels on different roads (see state road SR202 and SR203). This study reveals that the exterior noise is highly dependent on the surrounding environment, and to estimate the performance of rumble strips in term of exterior noise, different approaches are needed.

SR	Design Dimensions (in.)				Vehicle Passing in Near Lane (L _{max} dBA)		Vehicle Passing in Far Lane (L _{max} dBA)		Rank Order: Quiet to Loud (25' far lane)
	Depth	Width	Length	Spacing	25'	50'	25'	50'	
SR 6	0.5	6.9	8	12	80	76	84	80	2
US 12	0.5	6.9	12	24	86	80	88	81	5
SR 14	0.5	6.9	10	12	89	81	93	91	8
SR 28	0.375	6.0	12	12	88	84	88	83	6
SR 97	0.375	6.0	8	18	86	82	86	80	4
SR 202	0.5	6.0	12	12	84	82	84	83	3
SR 203	0.5	6.0	12	12	88	90	89	93	7
SR 410	0.375	6.0	8	12	81	76	82	77	1
SR 507	0.375	6.0	12	12	92	86	96	90	9

Note: SR 202 and SR 203 were based on WSDOT Standard Plans that allow a depth of 1/2-5/8.

Figure 3.1: Exterior noise measurements from different rumble strips on different road sites. [From Sexton T.V., 2014].

3.3 TERHAAR E., “RUMBLE STRIP NOISE EVALUATION”, MNDOT, 2015

In this publication the authors compared three rumble strip designs, one cylindrical and two sinusoidal using three vehicle types, a passenger, a pick-up and a semi-truck vehicle (only for the two sinusoidal designs) under three different speeds, 30, 45 and 60mph. The results from the report showed a decrement on exterior sound level for the sinusoidal designs (Fig 3.2). However, not all of the examined sinusoidal rumble strips achieve the recommended interior noise levels as shown in Figure 3.3.

The authors also examined when a sound can be detectable from the surrounding ambient noise and introduce a parameter called “Detectability”, a concept borrowed from a report by the US Army Tank Automotive Command (Fidell S. and Bishop D, 1974). Detectability is related to the frequency spectrum, and it has been observed that a sound can be detectable if any of its frequencies has a level at least 7 dBA higher than the same frequency in the ambient noise. The threshold of the 7 dBA is called the “Detectability factor”. An important detail regarding the detectability factor is that this sound level difference was calculated for active listening, which refers to when listeners are carefully trying to detect a change in sound.

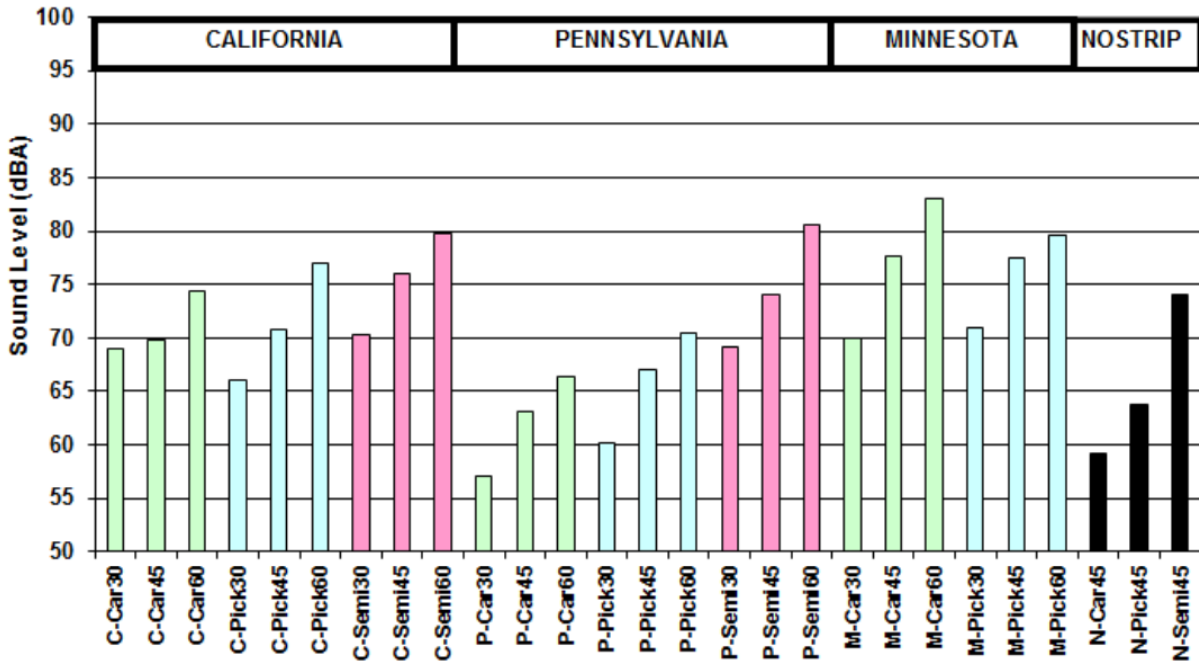


Figure 3.2: Exterior noise measurements for California (sinusoidal), Pennsylvania (sinusoidal) and Minnesota (cylindrical) designs. [From Terhaar and Braslau, 2015].

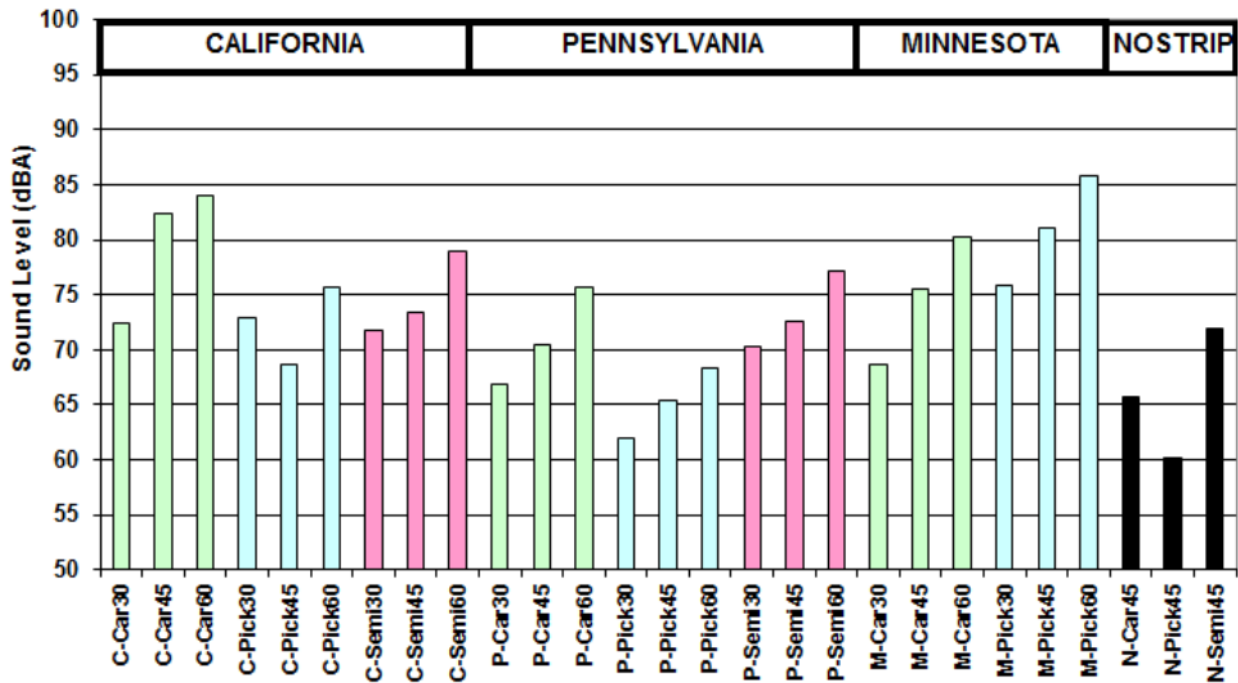


Figure 3.3: Interior noise measurements for California (sinusoidal), Pennsylvania (sinusoidal) and Minnesota (cylindrical) designs. [From Terhaar and Braslau, 2015].

The next two publications are not directly connected with rumble strip exterior noise. The reason these papers are reviewed and discussed is to demonstrate emerging methods in the field of

transportation, which include computer modeling and simulation, and to highlight how results are achieved using physical-based methods. Furthermore, these methods of experimentation allow the combination of analysis techniques, multiple design tests, and interchange of multiple parameters within experiments that would be challenging to test using field measurements in a cost-effective manner.

3.4 WANG BINXING ET AL., "ACOUSTIC MODELLING AND ANALYSIS OF VEHICLE INTERIOR NOISE BASED ON NUMERICAL CALCULATION", 2010

This report investigates vehicle cabin interior noise. It utilizes finite element analysis (FEA) and boundary element analysis (BEA) to analyze structures that support low frequencies, statistical energy analysis (SEA) to examine high frequency levels, car panel acoustic contribution analysis (PACA) to identify which panels from the interior of the vehicle’s cabin contribute more to the overall noise level and transfer path analysis (TPA) to identify the path which the acoustic energy travels to reach the driver’s ear. Figure 3.4 shows results before and after optimization of the cabin interior panels. Note that from this optimization, 3 - 5 dB noise reduction was observed at the frequencies of interest.

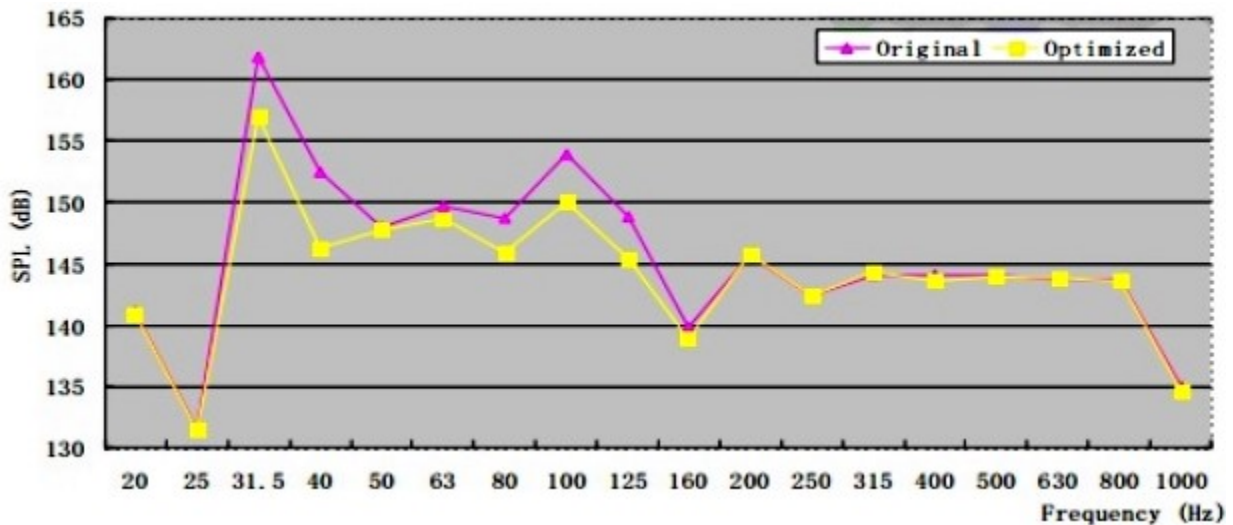


Figure 3.4: Before and after optimization frequency levels. [From Wang Binxing et al. 2010]

3.5 KIM ET AL., "DESIGN AND EVALUATION OF MODIFIED CENTERLINE RUMBLE STRIPS", NDOR, 2017

The authors created a 2D model of a tire and a road pavement with a rumble strip to examine the stress forces that are concentrated on the pavement while a tire rolls on rumble strips (Fig. 3.5). The study examines Nebraska’s current design along with three new designs. The results show that one of the new designs has lower pavement stress force concentration by 56% compared to Nebraska’s current design. In other words, installing this new design on pavements will result in

less road deterioration. However, the models for this study are not empirically validated, so field tests are needed to confirm these results.

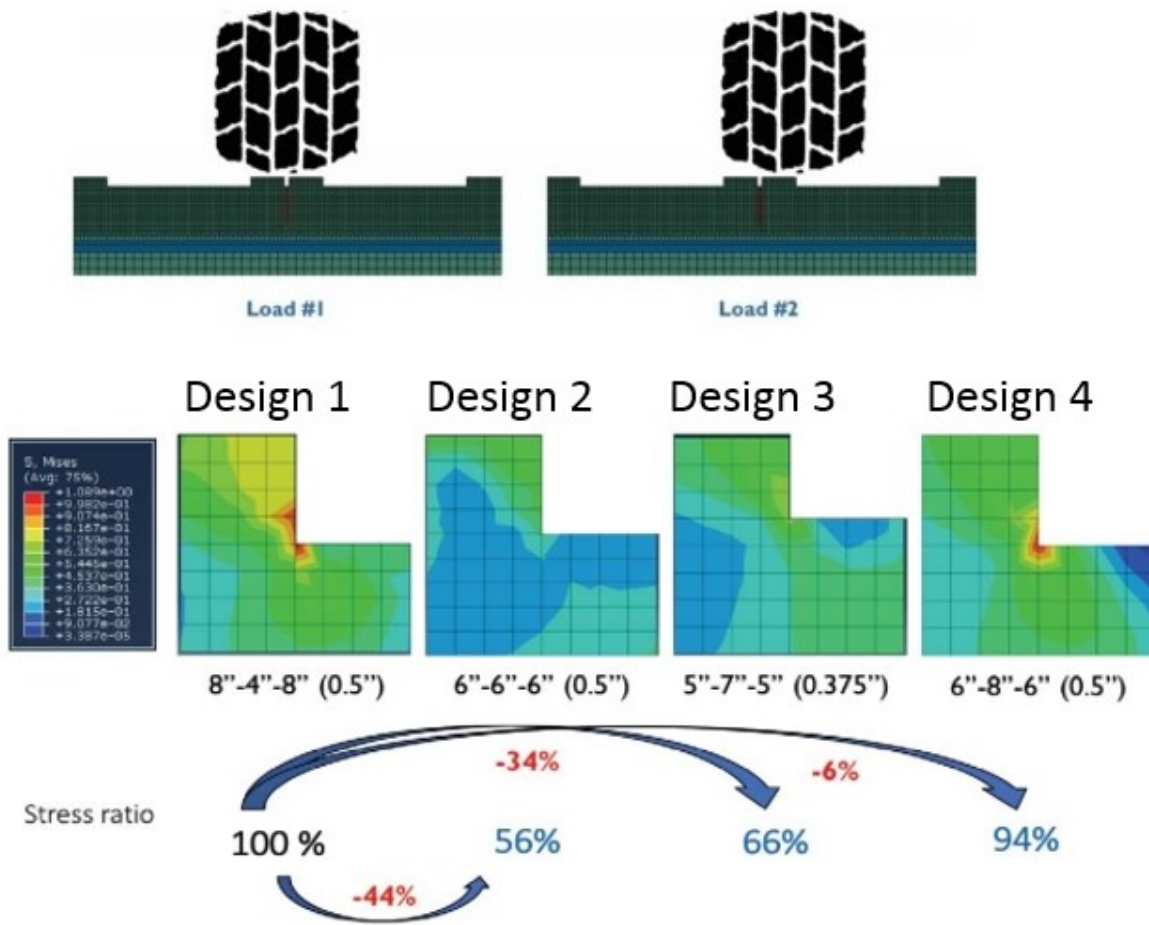


Figure 3.5: 2D modeling and visualization of the stress forces on four rumble strip designs. [From Kim et al., 2017].

4.0 THE FEA APPROACH

This section analyzes how information from the literature was applied to create, model, simulate, and evaluate twenty new rumble strip designs using finite element analysis (FEA). For all rumble strip designs that are simulated, length is assumed to be greater than the tire width. For the implementation discussion, the recommended length is above 12” to include consideration for truck tires, which have width equal to or greater than 12”. The speed for the simulations are 37.3 mph (60 Km/h).

4.1 RUMBLE STRIP PROFILE DEVELOPMENT

Three main profile categories were identified for further development including the “Rectified Sinusoidal (RS)”, “Sinusoidal (SS)” and “Sawtooth (ST)” profiles (Fig. 4.1). The RS and the SS profiles are symmetrical for all wavelengths. However, the RS profile has more aggressive slope than the SS profile, so the expectation is that RS will create more exterior noise than SS. The ST design is asymmetrical having its low section moved at the beginning of the profile creating a “fall of the cliff” scenario. The expectation is that the asymmetry will allow the profile to maintain a high vibrational feedback reducing at the same time its exterior noise level due to the low slope that follows.

Based on the three main profile categories, twenty rumble strip designs were created by changing the depth and wavelength. We tested the RS designs with wavelengths 14”, 19” and 24”, the SS designs with 14”, 16”, 19”, 24” and the ST designs with 15”, 20”, and 25”. All different wavelengths were tested at depth of 0.5” and 0.625”.

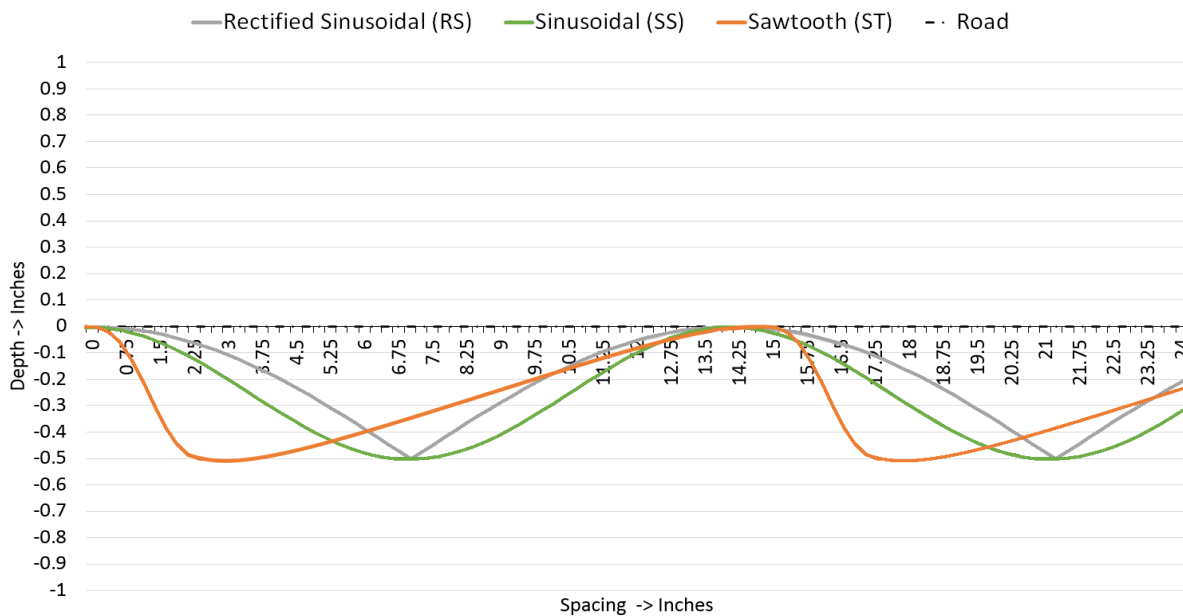


Figure 4.1: The three main rumble strip profile categories

4.2 CALCULATION PROCEDURE

Evaluation of the rumble strip profile includes several steps, which are explained in this section and depicted in Figure 4.2. The modeling and simulation of each design were implemented using Abaqus Unified FEA, which is a simulation product suite from the company Dassault Systems. The first step was to create the 3D FEA models for the tire and the road profiles. Then the materials, forces, and boundary conditions that are involved with the model interaction were defined (Fig. 4.2).

The analysis used for this simulation is called “static state analysis.” For this type of analysis, the tire rolls at a static position while the road below the tire changes position. The measurement for the level of each frequency was evaluated at five positions. The frequency range where these levels were extracted was 20-500Hz with a 5Hz interval.

The post-processing of the simulation results was performed using Microsoft Excel. The dB values for every frequency from each position were aggregated. A-weight reduction was then applied to the resulted dB value forming dBA values for each frequency. Then the 1/3 octave frequency bands were calculated and the dBA values for each band were estimated. The last step was to calculate the total dBA value for the specific rumble strip design and visualize its 1/3 octave analysis frequency spectrum.

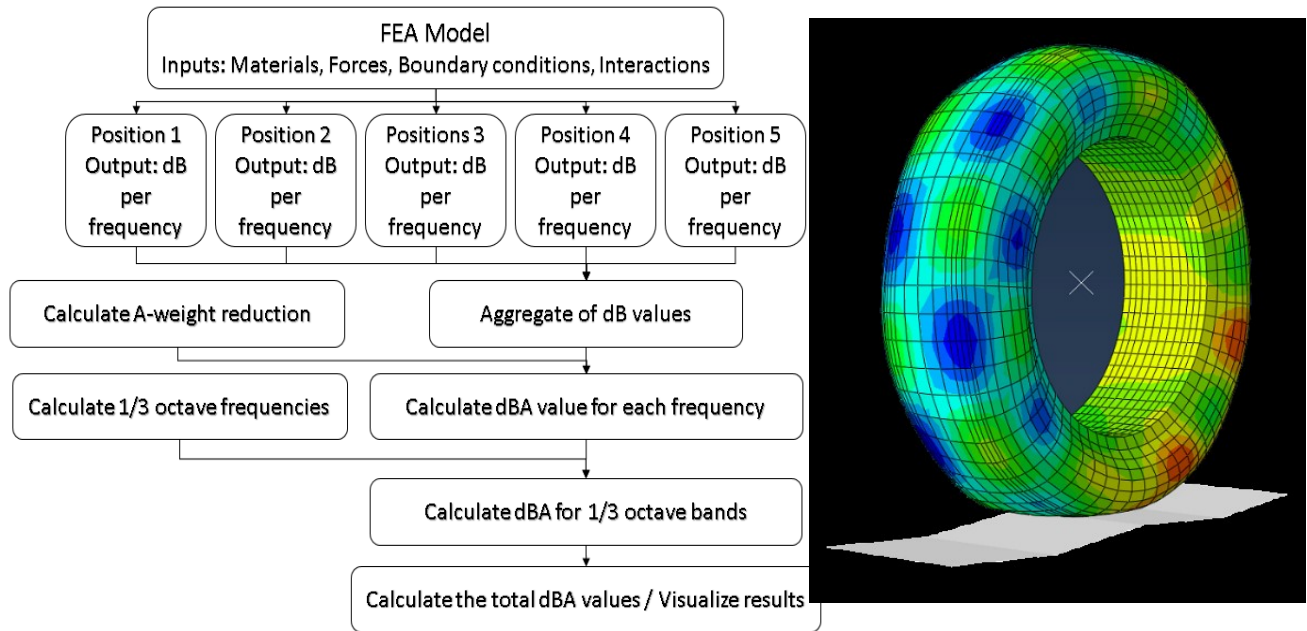


Figure 4.2: Flowchart of computation framework (left), 3D modeling of the tire and road (right).

5.0 RESULTS

5.1 COMPARISON AMONG THE 20 DESIGNS

Figure 5.1 shows the total dBA values for all simulated designs. As expected the rectified sinusoidal designs showed the highest noise levels followed by the sinusoidal designs and lastly, the sawtooth designs which presented the lowest dBA levels. Additionally, the estimations that deeper rumble strips will have higher feedback were also correct using this modeling approach. The chart reveals a correlation between wavelength and dBA values whereby as the wavelength increases the dBA level decreases.

The 1/3 octave analysis frequency spectrum for each design can be seen in Figure 5.2 (and Appendix A). An overall observation is that profiles with short wavelength tend to create complex frequency spectrum with peaks starting from low frequencies such as 79Hz expanding higher up to 315 and 400Hz. In contrast, designs with longer wavelengths seem to reduce their high frequency content and result in a smooth frequency spectrum, which is closer to the reference (flat road) frequency spectrum.

Most of the rectified sinusoidal and the sinusoidal designs showed strong peaks at the frequency of 79Hz. Rectified sinusoidal designs also showed excitations at 125, 315 and 400Hz. Sawtooth designs showed lower levels than rectified sinusoidal and sinusoidal at the lowest frequency peak of 79Hz. Sawtooth designs showed higher peaks at 125Hz but with dBA levels lower than what rectified sinusoidal and sinusoidal have at 79Hz.

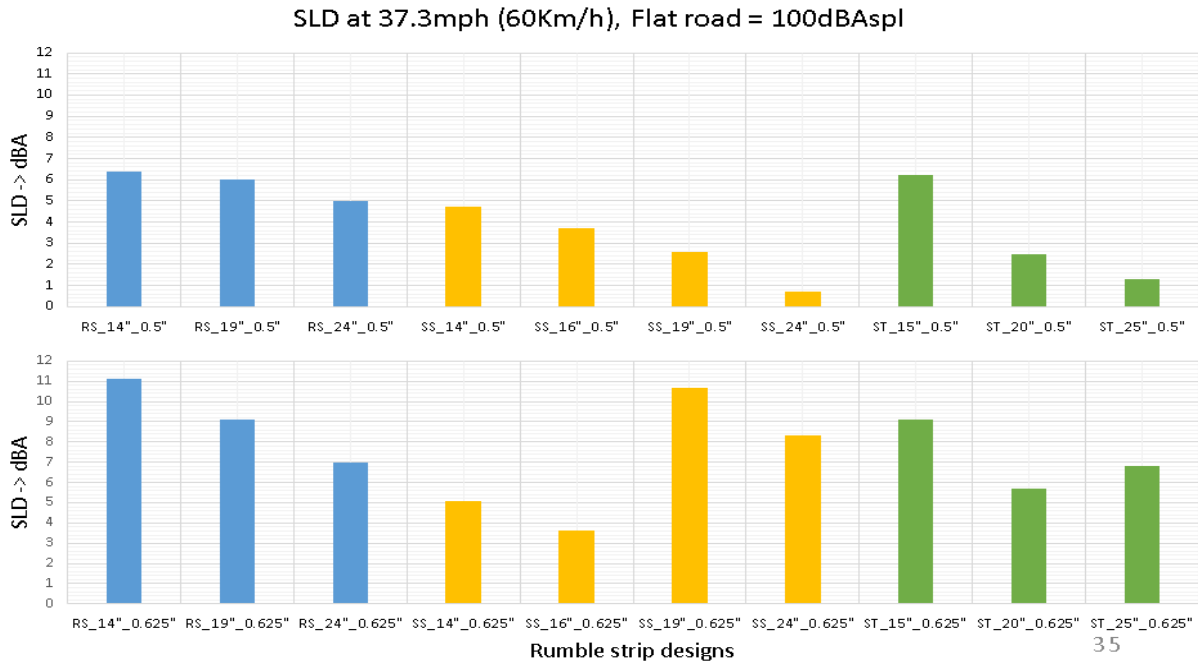


Figure 5.1: dBA values for each design category RS, SS and ST. Top row is for 0.5" depth and bottom is for 0.625" depth. The middle number is wavelength

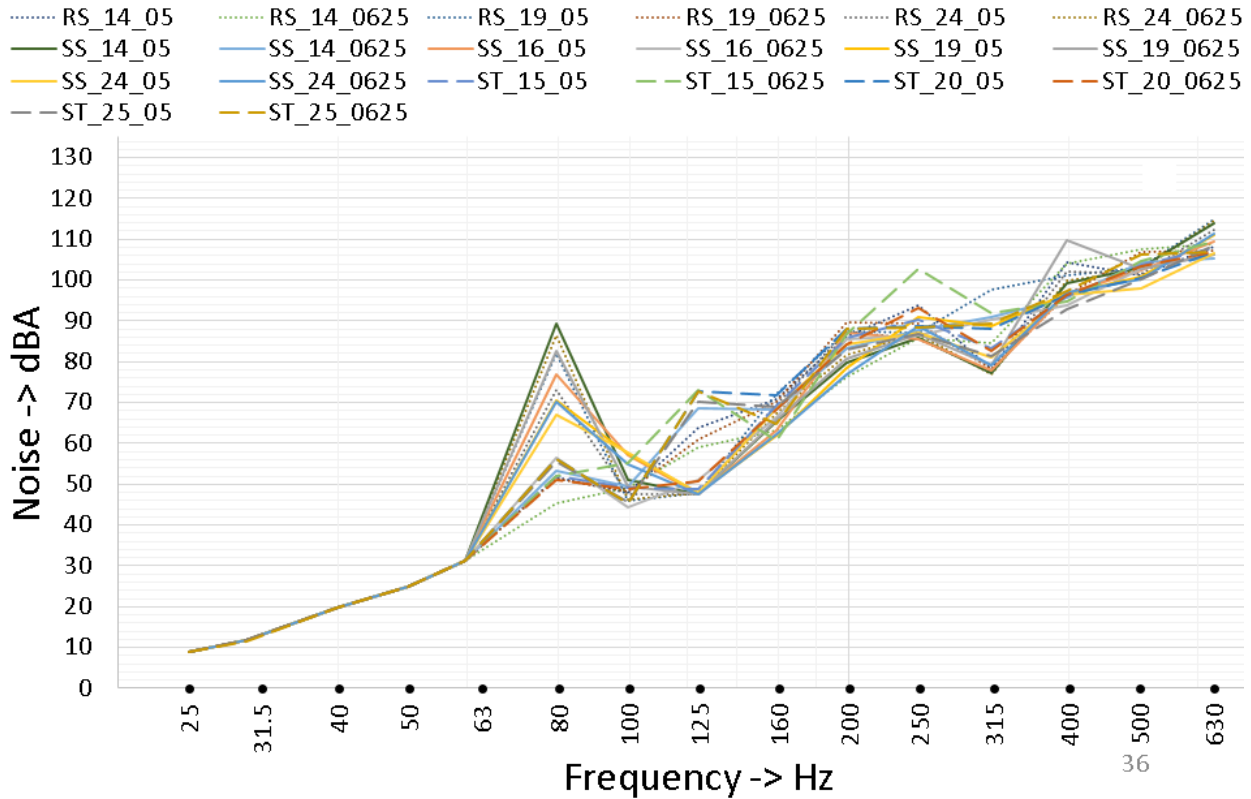


Figure 5.2: 1/3 octave analysis frequency spectra for all the simulated designs. Please also refer to Appendix A for individual analysis.

5.2 SIX SELECTED RUMBLE STRIP DESIGNS

Based on the results from 20 modeled designs, six patterns were selected. These designs along with their SLD dBA levels are illustrated in Figure 5.3. There are three sinusoidal and three sawtooth designs in the selected list, and Figure 5.3 illustrates that these six designs present lower noise levels than published measurements in the literature. The selection criteria for these six designs included the dBA level that the specific designs produce, combined with their frequency spectrum profiles focusing on low frequency output. As explained earlier, low frequencies travel further, thus the selected designs have lower peaks in the low frequency range.

Another criterion for the design selection was the geometry of each design. On short wavelength designs, the simulated tire did not have contact with the pavement at the lower section of the rumble strip. The air in those cavities will get pressurized and de-pressurized as the tire rolls, therefore becoming a sound source for exterior noise. Additionally, when the tire does not follow the whole wavelength track, the vertical displacement decreases, and the vibrational feedback decreases as well (Miles and Finley, 2007).

Lastly, some of the designs tested in this analysis have been installed and tested as field tests in the literature, so even though they might have lower dBA values, it is known that they also have insufficient interior level, which makes them unsuitable for alerting the drivers (Donavan and Rymer, 2015, Terhaar and Braslau, 2015, Terhaar et al., 2016).

Reference (Flat road) level = 100 dBA at 37.3mph (60Km/h),

Approx. SLD for cylindrical rumble strip design (15.3dBA @ 25 feet)

Approx. SLD for sinusoidal rumble strip design (11.6dBA @ 25 feet)

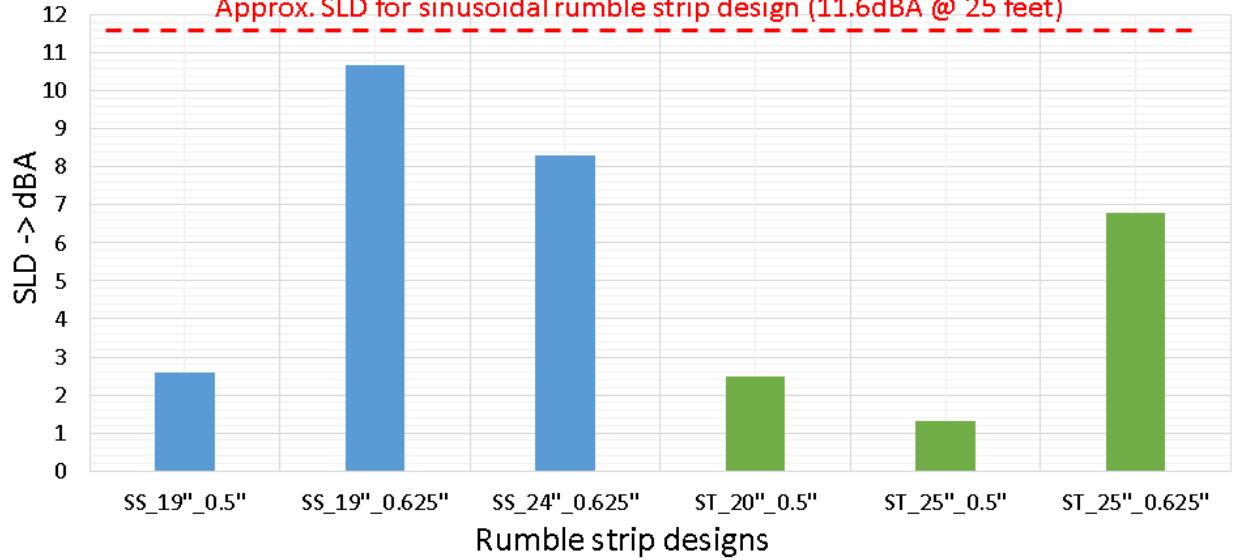


Figure 5.3: dBA values for all the six suggested designs

--- Flat road — SS_24_0625 — SS_19_0625 — SS_19_05

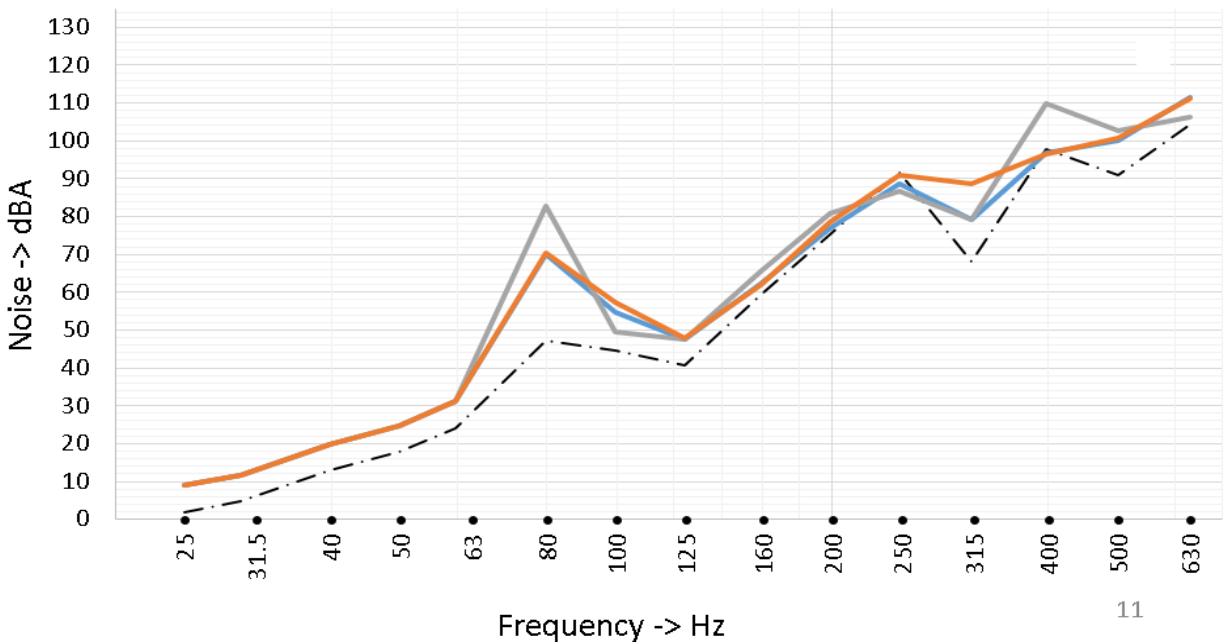


Figure 5.4: 1/3 octave frequency spectra for flat road and the sinusoidal designs

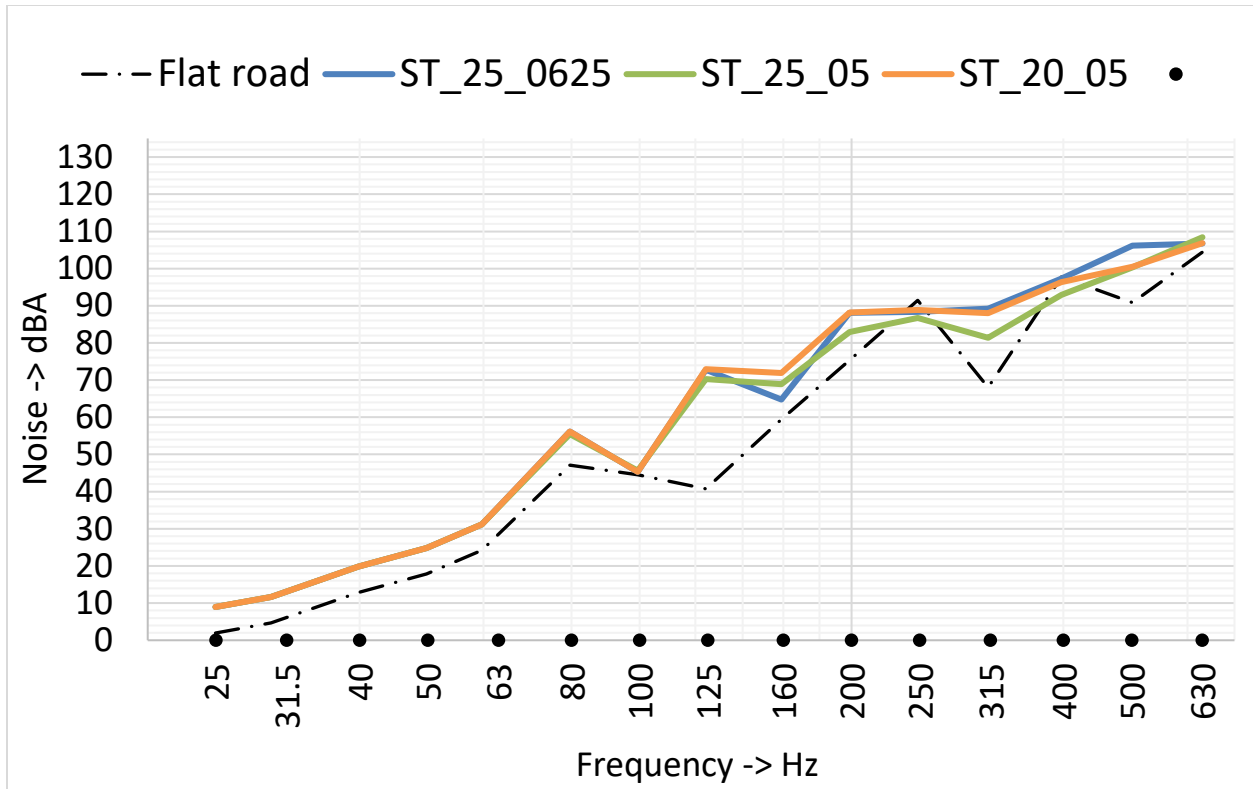


Figure 5.5: 1/3 octave frequency spectra for flat road and the sawtooth designs

5.3 NOISE CONTOUR MODELING FOR VISUAL ANALYSIS OF RUMBLE STRIP DESIGN IMPACTS

A secondary goal of this project was to investigate the ability to use outdoor sound propagation modeling to visually assess the effects of different rumble strip designs in terms of the modeled sound levels at nearby residential areas. Sound propagation models implemented in available software provide a means of generating noise contour maps for complaint locations. Due to the power of maps as tools for communication, visualization, and decision support (e.g., Alcorn, 2000; Zerger, 2002), it is envisaged that these noise contour maps may be useful in analyzing and communicating the impacts of different rumble strip designs internally (i.e., within ODOT) and externally (i.e., with other State DOTs, FHWA, and/or external stakeholders).

For this portion of the project, it was deemed beneficial to test the sound propagation modeling software tools on an actual complaint location. Therefore, as a first step, the project team obtained from ODOT a list of four complaint locations:

1. La Grande area: I84 between MP 259 and 261
2. Parkdale area: Hwy 281 (Hood River Hwy) near Mile Point 13.76 (later confirmed by ODOT to have been removed)
3. McMinnville area: OR 154 near Mile Point 2.4

4. Corvallis area: OR-99W near 70.12 and 69.32

From these identified sites, the next step was to select a single location as the focus area for this portion of the analysis. To make this selection, each site was analyzed for: a) existing shoulder rumble strips (important for linking this work with ODOT SPR 800, “Quantifying the Performance of Low-Noise Rumble Strips”); b) nearby residences; and c) a range of terrain and vegetation (important for testing different input parameters to the sound propagation algorithms). Based on these criteria, Location 1 (La Grande area) was selected as the project site. Analysis performed in ArcGIS and in Google Earth (Figure 5.6) indicated the presence of residences within 200-600 feet of the shoulder rumble strips installed on I-84 within the project site. Additionally, the La Grande location was found to contain a range of terrain and vegetation within a 1.0 square mile area (~100-ft elevation range with trees over 40-ft AGL).



Figure 5.6: Analysis of La Grande project site in Google Earth.

Having identified the project site, the next step was to obtain available data for the site needed to generate the inputs to the sound propagation modeling software. Topographic data for the site was obtained in the form of a high-resolution digital elevation model (DEM) from the Oregon Department of Geology and Mineral Industries (DOGAMI), and available on the NOAA Data Access Viewer (<https://coast.noaa.gov/dataviewer/#/lidar/search/>). The source data was collected for DOGAMI by Watershed Sciences, Inc. (currently Quantum Spatial) using Leica ALS50 Phase II and ALS60 airborne topographic lidar systems to meet a point density specification of ≥ 8 points per square meter (Watershed Sciences, 2011). A portion of the lidar point cloud is shown in Figure 5.7. Meteorological data was obtained from Weather Spark and used to generate monthly averages of wind speed and direction, temperature, humidity and atmospheric pressure. Additionally, land cover data was obtained from USGS’s National Gap Analysis Program (GAP) Land Cover Viewer (USGS, 2015).

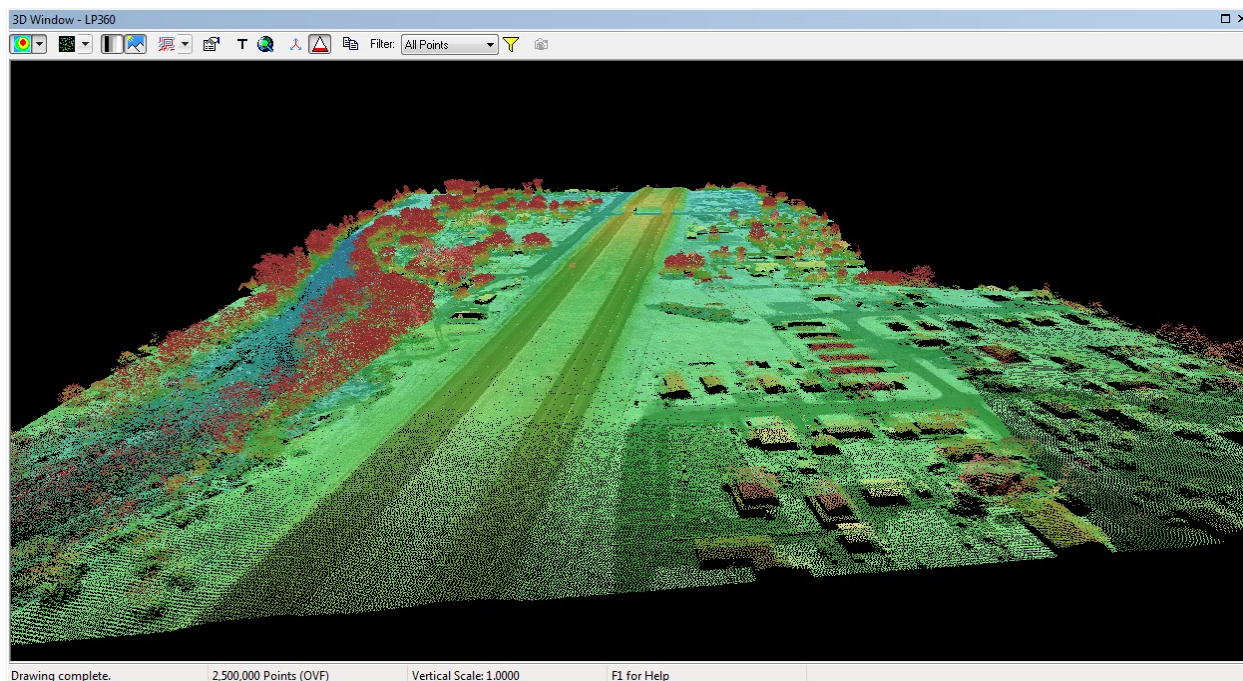


Figure 5.7: DOGAMI lidar point cloud data for La Grande project site viewed in QCoherent’s LP360 software.

The next step was to identify and obtain sound propagation modeling software for use in this project. Three alternatives were considered: 1) FHWA’s Traffic Noise Model (TNM ®) Version 3.0 (with GUI and interoperability functionality developed by Gannet Fleming), 2) NMSim (Noise Model Simulation) developed by Wyle Labs and used by the National Park Service (NPS); and 3) SPreAD-GIS, which is based on the System for the Prediction of Acoustic Detectability (SPreAD) algorithm of Harrison et al. (1980) and implemented as an ArcGIS toolbox by Reed et al. (2010). Each software package considered uses an outdoor sound propagation model that accounts for spreading loss, atmospheric absorption (a function of temperature and humidity), meteorological conditions, ground (absorption and scattering by vegetation, and terrain and manmade objects) and other parameters, and has additional functionality deemed by the project team to be beneficial for this project. TNM was considered a promising option, due to its use by FHWA and State DOTs for highway noise modeling (Bajdek et al., 2015). However, TNM 3.0 was not available to the project team during this study. Of the other two options, SPreAD-GIS was selected for use in this project, due to its compatibility with the GIS mapping application used by the project team, ease of use, ready-access (free web download), and the user-selectable options available in its noise contour mapping functionality.

The SPreAD-GIS software was run by the project team on a Windows desktop (Hewlett Packard HP Z230, 32 GB RAM, with Intel ® Core i7-4790 CPU at 3.6 GHz, running Windows 7). Input to the SPreAD-GIS model runs is shown in Table 5.1. The output noise contour maps generated with SPreAD-GIS are shown in Figures 5.8-5.9. It should be noted that while only static displays of the noise contour maps are feasible in this report, the differences in noise contours resulting from the different rumble strip designs are best viewed using a “flicker” utility with a GIS to

quickly alternate between the contours produced using the inputs corresponding to the different designs. These GIS data layers are available from the project team upon request.

Table 5.11: Input to SPreAD-GIS Model Runs.

User-Input Parameter	How obtained
Noise level in dBA for each rumble strip design	Mean of model output described above for each rumble strip design
Elevation data set (digital elevation model or digital surface model)	DOGAMI lidar available through NOAA’s data distribution portal
Sound frequency	Assumed 250 Hz
Distance from source	Assumed 1 ft (minimum value in SPreAD-GIS)
Temperature	85 °F = mean for La Grande area in month of August, as computed from meteorological data
Humidity	47% = mean for La Grande area in month of August, as computed from meteorological data
Wind direction	315° = mean for La Grande area in month of August, as computed from meteorological data
Wind speed	7 mph = mean for La Grande area in month of August, as computed from meteorological data

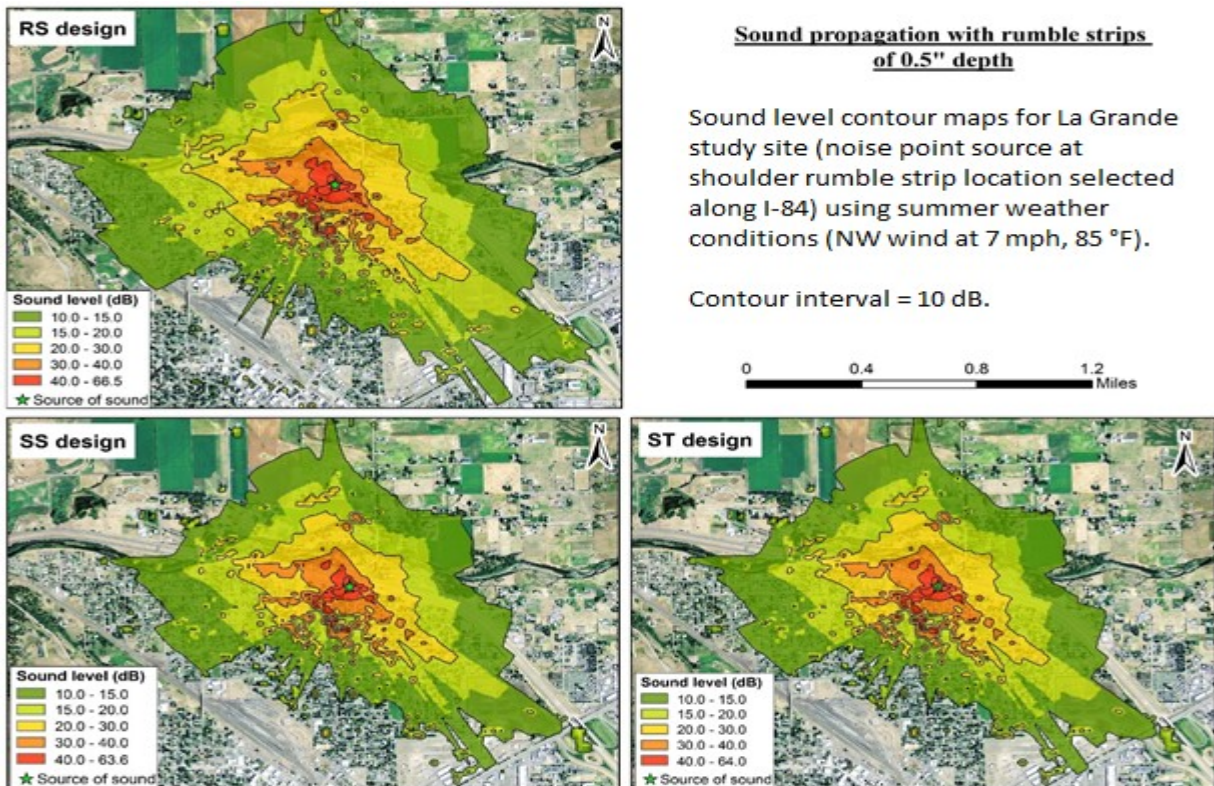


Figure 5.8: Noise contour maps based on mean sound levels for three rumble strip design categories (rectified sinusoidal - RS, sinusoidal - SS, and sawtooth - ST) with 0.5" depth for La Grande project site.

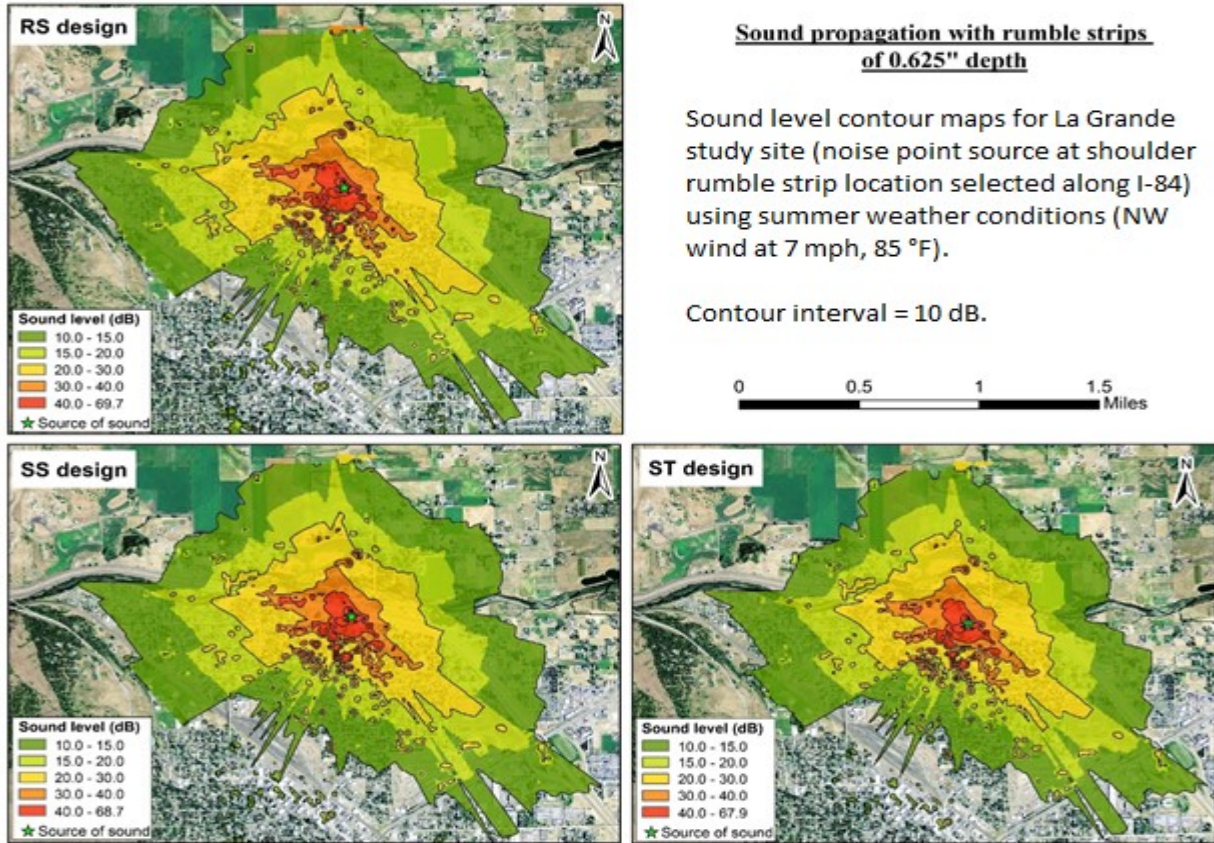


Figure 5.9: Noise contour maps based on mean sound levels for three rumble strip design categories (rectified sinusoidal - RS, sinusoidal - SS, and sawtooth - ST) with 0.625" depth for La Grande project site.

Analysis of the output noise contour maps shows that, for the 0.5" depth, the sawtooth and sinusoidal designs result in similar contours, with the rectified sinusoidal designs leading to noticeably larger contour areas with higher sound levels in some residential areas. For the 0.5" depth, the sinusoidal designs result in very slightly smaller contour areas than the sawtooth designs. For the 0.625" depths, the same general trends are observed, but with the sawtooth designs producing the smallest contour areas. Although it is recommended to use caution in evaluating the output of this modeling, due to limitations of both the underlying models and inputs, a clear conclusion from this portion of the study is that noise contour modeling is an effective tool for visually assessing and communicating the impacts of rumble strip design selection. A recommendation for future work is to investigate use of FHWA's Traffic Noise Model (TNM) v3.0, which includes GIS interface capabilities, as well as functionality for generating sound level contours (est. FHWA, 2019).

6.0 CONCLUSION

The purpose of this project was to develop new low exterior noise rumble strip designs based on informed exterior noise criterion. After an in-depth literature review, limitations of using published exterior noise data for modeling new rumble strip patterns became apparent, highlighting the need for a new design approach. However, the literature review did provide key design parameters that were then leveraged to inform computer modelling and simulation using 3D finite element static state analysis. Out of twenty tested designs, six new rumble strip patterns with predicted lower exterior noise output were identified for future field testing.

In sum, this study presents a physics-based method of evaluating rumble strips based on the modeled output of exterior noise. This method is in-line with emerging modeling trends previewed in the literature review, and showcases the utility of this approach given the large number of designs that were evaluated given the limited funding of this project. Furthermore, this study also incorporates a valuable communication tool using noise contour mapping for improved noise visualization of rumble strip installation near communities.

7.0 FUTURE WORK

This study was an initial step in utilizing physical-based methods for testing rumble strips. It provided preliminary results; however, limitations of this work need to be considered. The designs were tested using one specific speed and the calculations were collected at five positions of the tire on the strip using a static state approach. In order to fully understand the behavior of a tire on rumble strip, a dynamic simulation is needed to capture every detail of the tire movement. Additionally, more parameters should be considered, including different speeds, vehicles, angles of departure and tire sizes.

Rumble strip modeling also needs to incorporate interior noise signals to ensure effectiveness. To simulate the sound path from the tire to the driver's ear while capturing the noise level at that position, a complete vehicle parameter model is required. Moreover, to receive a comprehensive overall feedback understanding, the tactile signals should be analyzed as well. The overall future goal is to develop road noise prediction models using finite element analysis with exterior and interior audible and tactile data, traffic volume and topological/environmental conditions.

8.0 REFERENCES

- Alcorn, J. B. (January 01, 2000). Borders, Rules and Governance: Mapping to catalyse changes in policy and management. *Gatekeeper Series International Institute for Environment and Development Sustainable Agriculture and Rural Livelihoods Programme*, 91.
- Bajdek, C., Menge, C., Mazur, R., Pate, A., & Schroeder, J. (2015). *Recommended Best Practices for the Use of the FHWA Traffic Noise Model (TNM)* (Publication). Washington, D.C.: Federal Highway Administration.
- CTC and Associates LLC, "*Traffic noise generated by rumble strips*". Caltrans Division of Research and Innovation, Dana York, Environmental Services, 2012.
- Donavan, P. R., & Rymer, B. (2015). Comparison of Vehicle Responses to Rumble Strip Inputs of Varying Design. *SAE International Journal of Passenger Cars - Mechanical Systems*, 8(3). doi:10.4271/2015-01-2274
- Engineering Acoustics/Outdoor Sound Propagation. (2018, December 8). *Wikibooks, the Free Textbook Project*. Retrieved October 26, 2017 from https://en.wikibooks.org/w/index.php?title=Engineering_Acoustics/Outdoor_Sound_Propagation&oldid=3497331.
- Fidell, S., & Bishop, D. E. (1974). Prediction of acoustic detectability Technical Report 11949. *Warren (MI): US Army Tank Automotive Command*.
- Harwood, D. W. (January 01, 1993). Use of rumble strips to enhance safety. *National Cooperative Highway Research Program Synthesis of Highway Practice*, 191, 1993.
- Harrison, R. T., Clark, R. N., & Stankey, G. H. (1980). *Predicting impact of noise on recreationists*. San Dimas, Calif: U.S. Forest Service, Equipment Development Center.
- Hobbs, J. (2018, January 12). Fletcher Munson Curve: The Equal Loudness Contour of Human Hearing. Retrieved from <https://ledgernote.com/columns/mixing-mastering/fletcher-munson-curve/>
- Kim, Y., You, T., & Rilett, L. (2017). *Design and Evaluation of Modified Centerline Rumble Strips* (Publication No. SPR-P1 (16) M034). Lincoln, NE: Nebraska Department of Roads Research Report.
- Miles, J. D., & Finley, M. D. (January 01, 2007). Factors that influence the effectiveness of rumble strip design. *Transportation Research Record*, 2030, 1-9.
- Octave Band Filters. (n.d.). Retrieved September 13, 2017, from <https://www.noisemeters.com/help/faq/octave-bands.asp>

- Personal Music Players & Hearing. (n.d.). Retrieved October 5, 2017, from https://ec.europa.eu/health/scientific_committees/opinions_layman/en/hearing-loss-personal-music-player-mp3/1-3/2-sound-measurement-decibel.htm
- Reed, S., Mann, J., & Boggs, J. (2009). *SPreAD-GIS: An ArcGIS toolbox for modeling the propagation of engine noise in a wildland setting* (Version 1.2, Rep.). San Francisco, CA: The Wilderness Society.
- Sexton, T. (2014). *Evaluation of Current Centerline Rumble Strip Design(s) to Reduce Roadside Noise and Promote Safety* (Tech. No. WA-RD 835.1). Olympia, WA: Washington State Department of Transportation.
- Smadi, O., Hawkins, N. R., United States., American Association of State Highway and Transportation Officials., & National Research Council (U.S.). (2016). *Practice of rumble strips and rumble stripes: A synthesis of highway practice*.
- Terhaar, E., Braslau, D., Minnesota., Wenck Associates, Inc., David Braslau Associates, Inc., & Minnesota Local Road Research Board. (2015). *Rumble strip noise evaluation*. St. Paul, Minn: Minnesota Department of Transportation, Research Services & Library.
- Terhaar, E., Braslau, D., Fleming, K., Wenck Associates, Inc., David Braslau Associates, Inc., Minnesota., & Minnesota. (2016). *Sinusoidal rumble strip design optimization study*. St. Paul, Minn: Minnesota Department of Transportation, Research Services & Library
- Torbic, D. J., Hutton, J. M., Bokenkroger, C. D., Bauer, K. M., Harwood, D. W., Gilmore, D. K., ... & Garvey, P. M. National Research Council (U.S.), National Research Council, American Association of State Highway and Transportation Officials, & USA. (2009). *NCHRP Report 641: Guidance for the design and application of shoulder and centerline rumble strips*. Washington, D.C: Transportation Research Board of the National Academies.
- Wang, B., Zheng, S., Zhou, L., Liu, S., Lian, X., & Li, K. (2010, 11-12 May 2010). *Acoustic Modelling and Analysis of Vehicle Interior Noise Based on Numerical Calculation*. Paper presented at the 2010 International Conference on Intelligent Computation Technology and Automation.
- Watershed Sciences. (2011). *LiDAR Remote Sensing Data Collection Department of Geology and Mineral Industries Umatilla* (Rep.). Portland, OR: Department of Geology and Mineral Industries.
- Wikipedia contributors. (2018, October 28). ITU-R 468 noise weighting. In *Wikipedia, the Free Encyclopedia*. Retrieved October 26, 2017, from https://en.wikipedia.org/w/index.php?title=ITU-R_468_noise_weighting&oldid=866109181
- Zerger, A. (January 01, 2002). Examining GIS decision utility for natural hazard risk modelling. *Environmental Modelling and Software*, 17, 3, 287-294.

**APPENDIX A: 1/3 OCTAVE ANALYSIS FREQUENCY SPECTRA FOR
THE TWENTY SIMULATED RUMBLE STRIP DESIGNS**

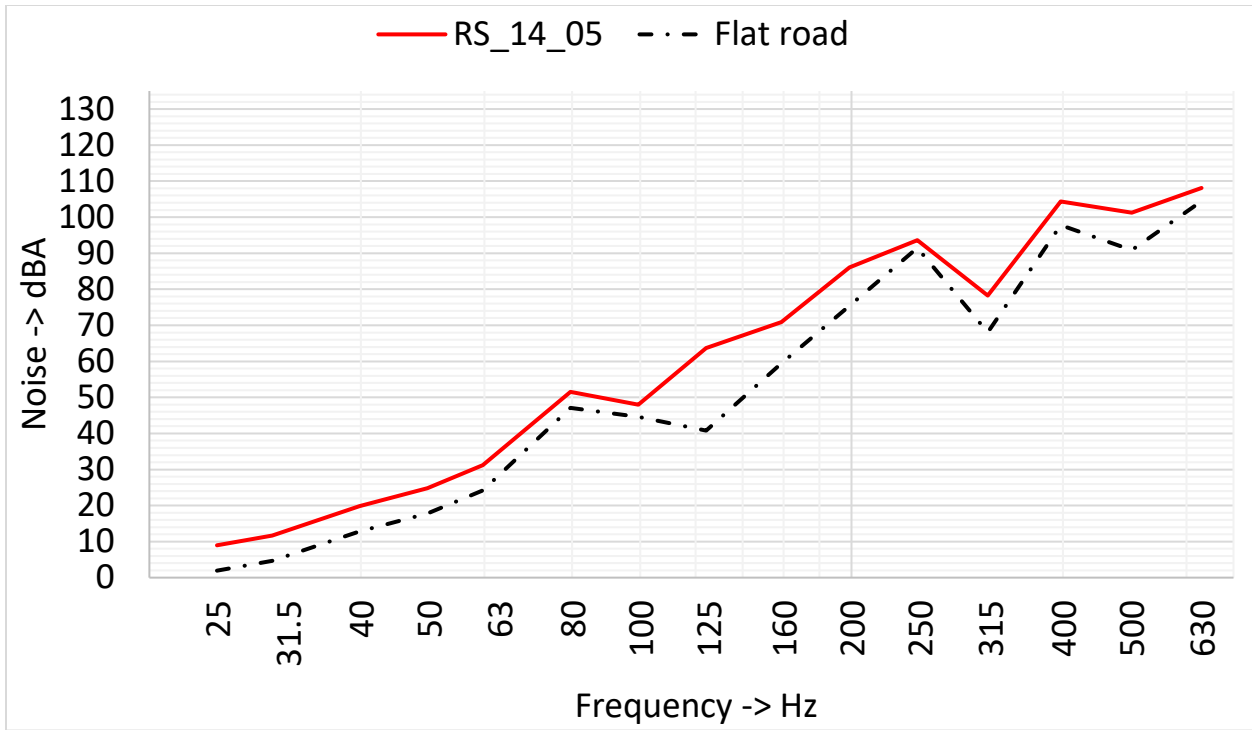


Figure A.1: 1/3 octave frequency spectrum for RS_14_05

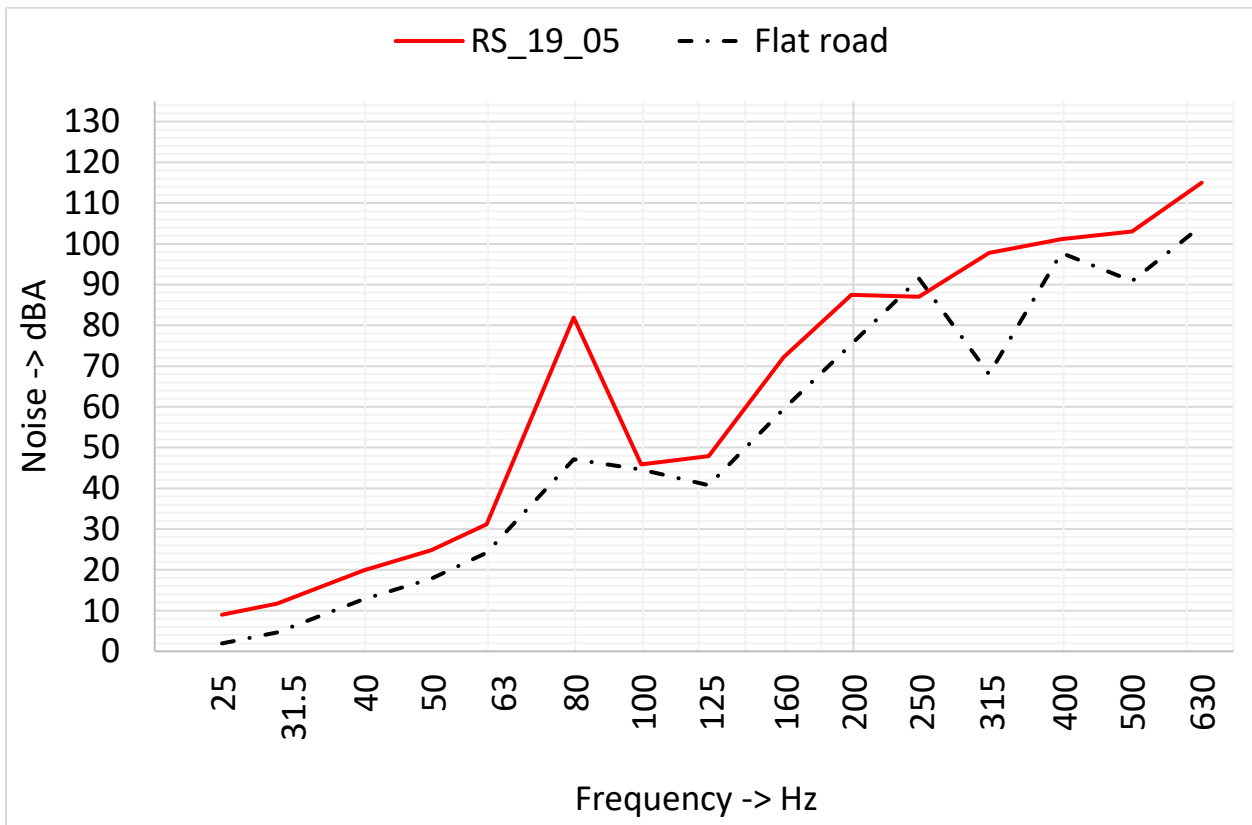


Figure A.2: 1/3 octave frequency spectrum for RS_19_05

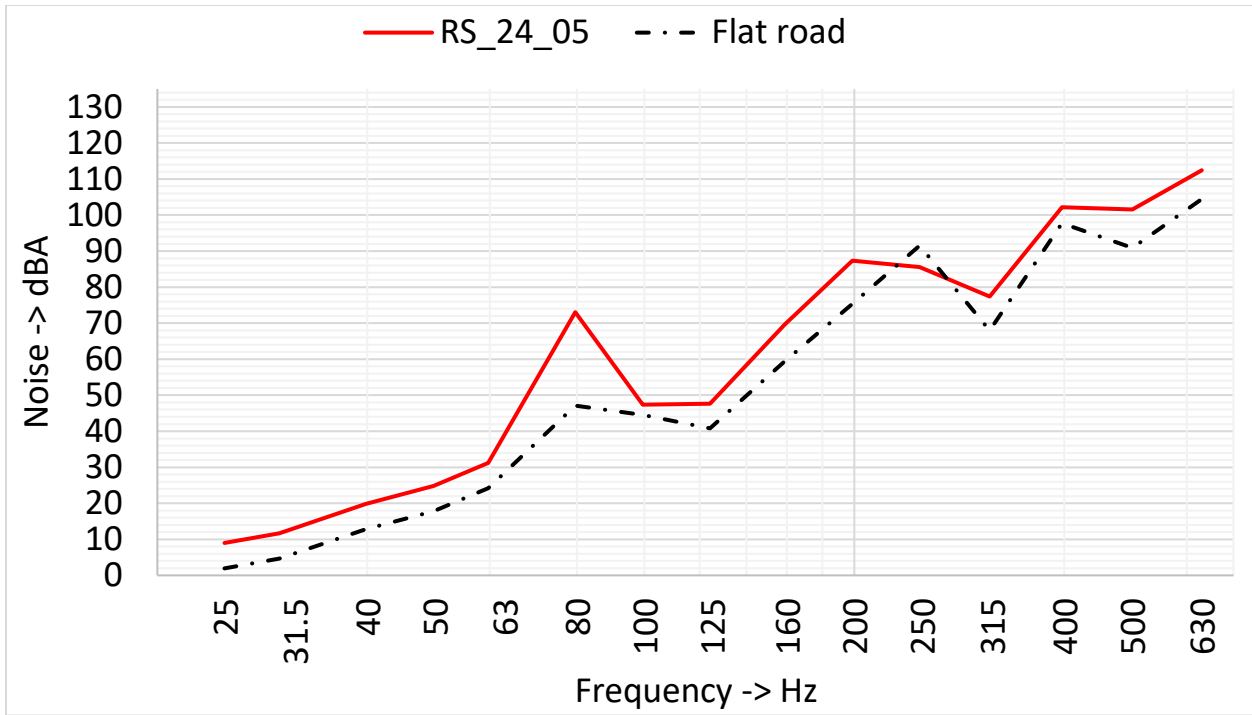


Figure A.3: 1/3 octave frequency spectrum for RS_24_05

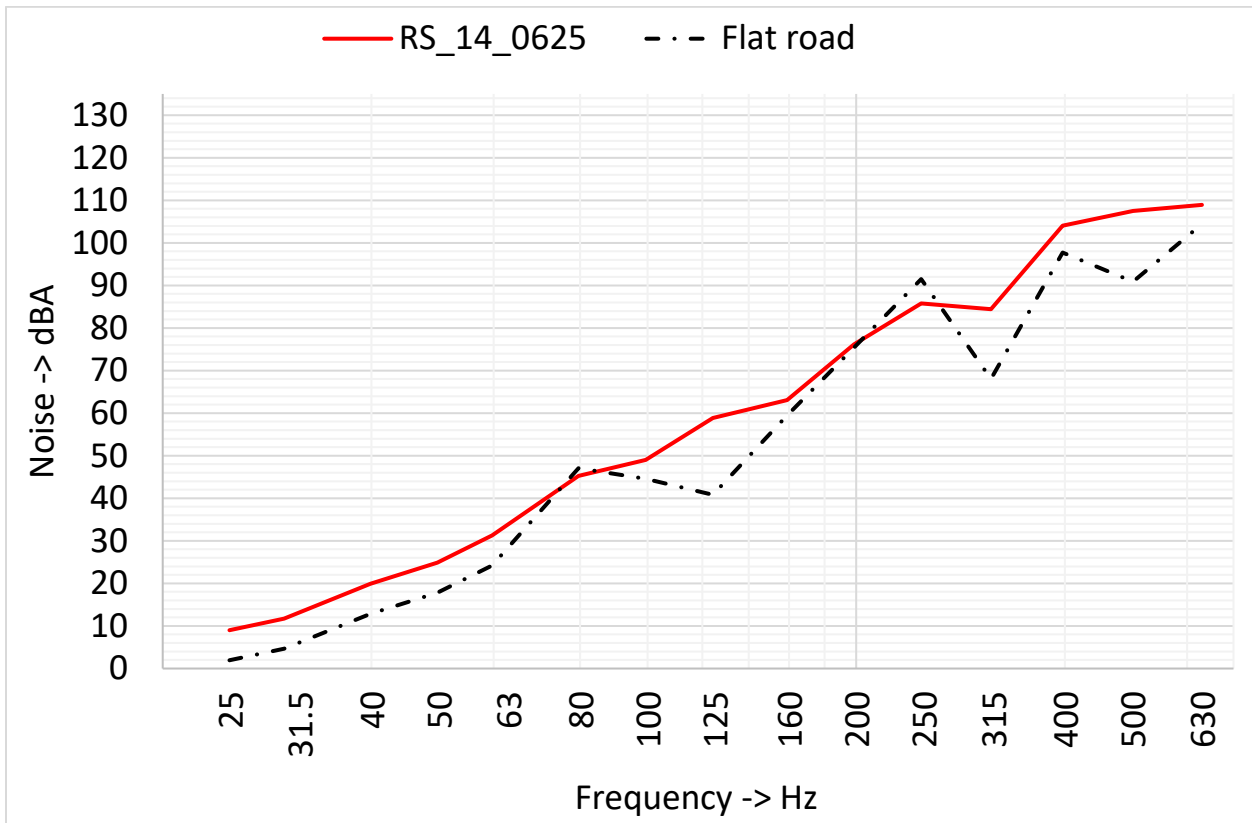


Figure A.4: 1/3 octave frequency spectrum for RS_14_0625

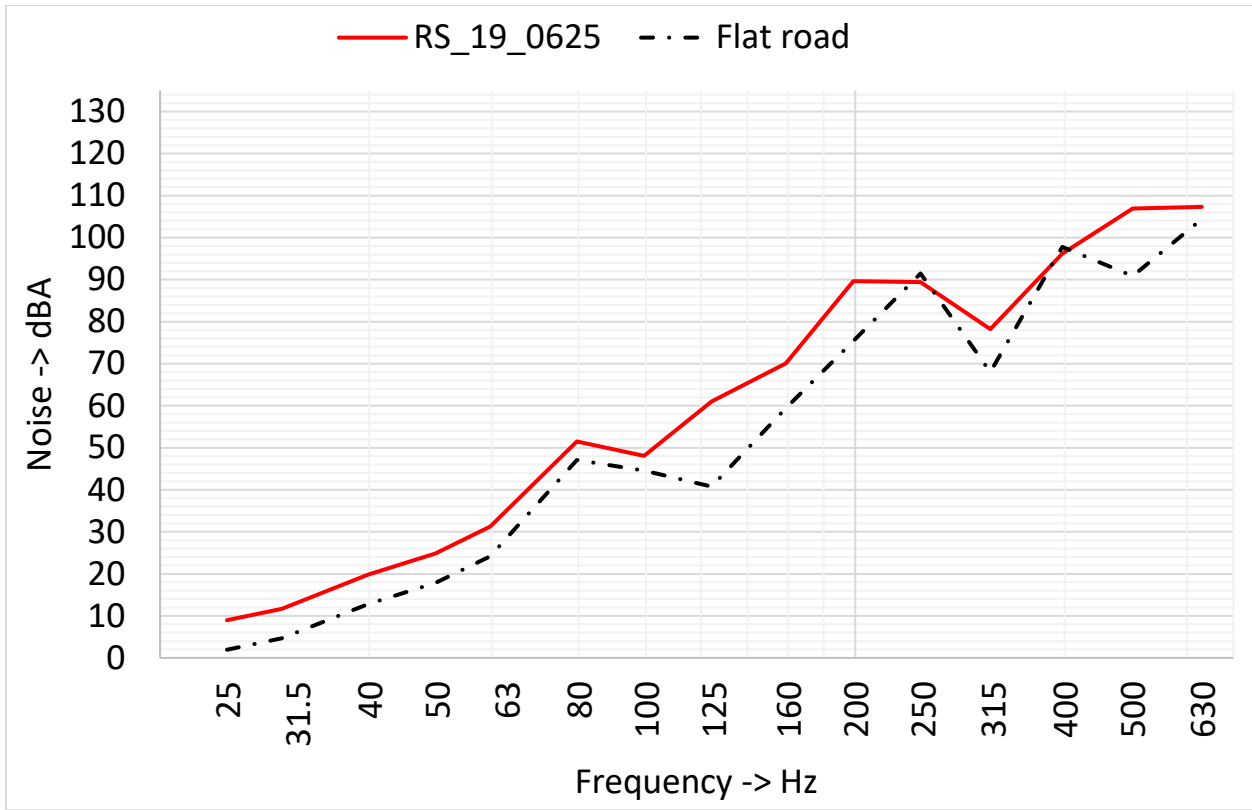


Figure A.5: 1/3 octave frequency spectrum for RS_19_0625

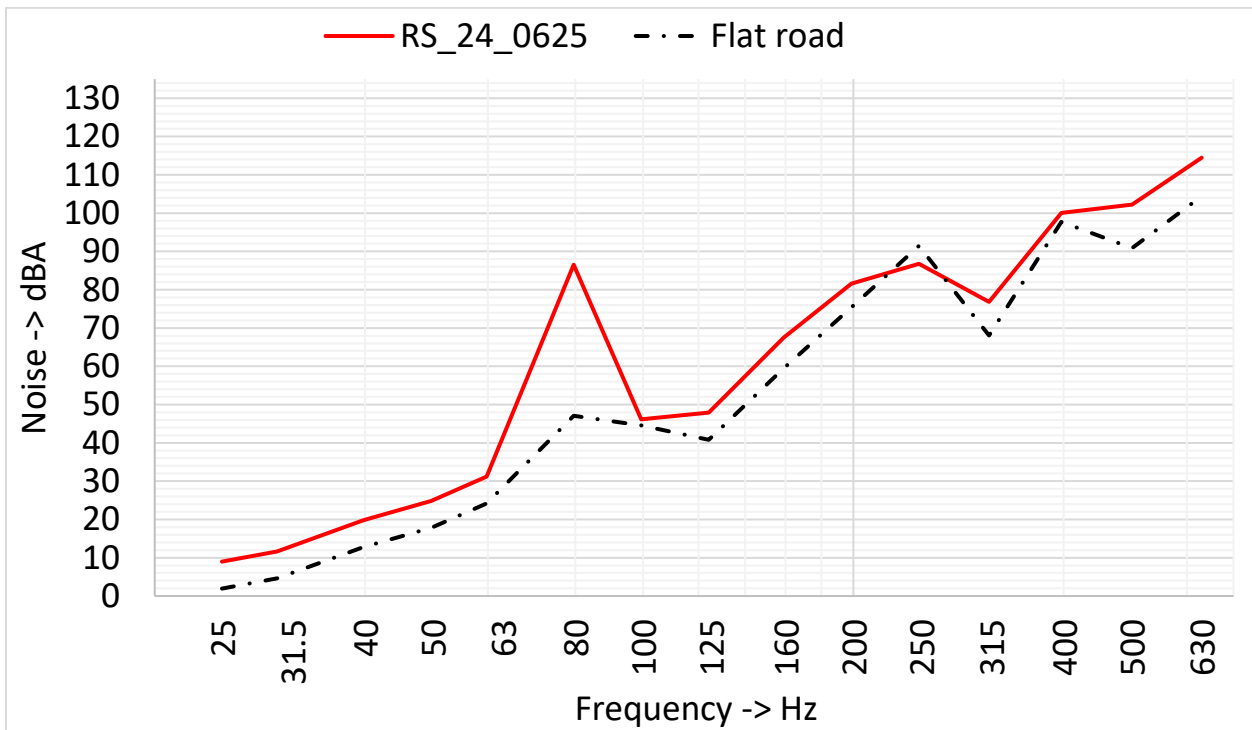


Figure A.6: 1/3 octave frequency spectrum for RS_24_0625

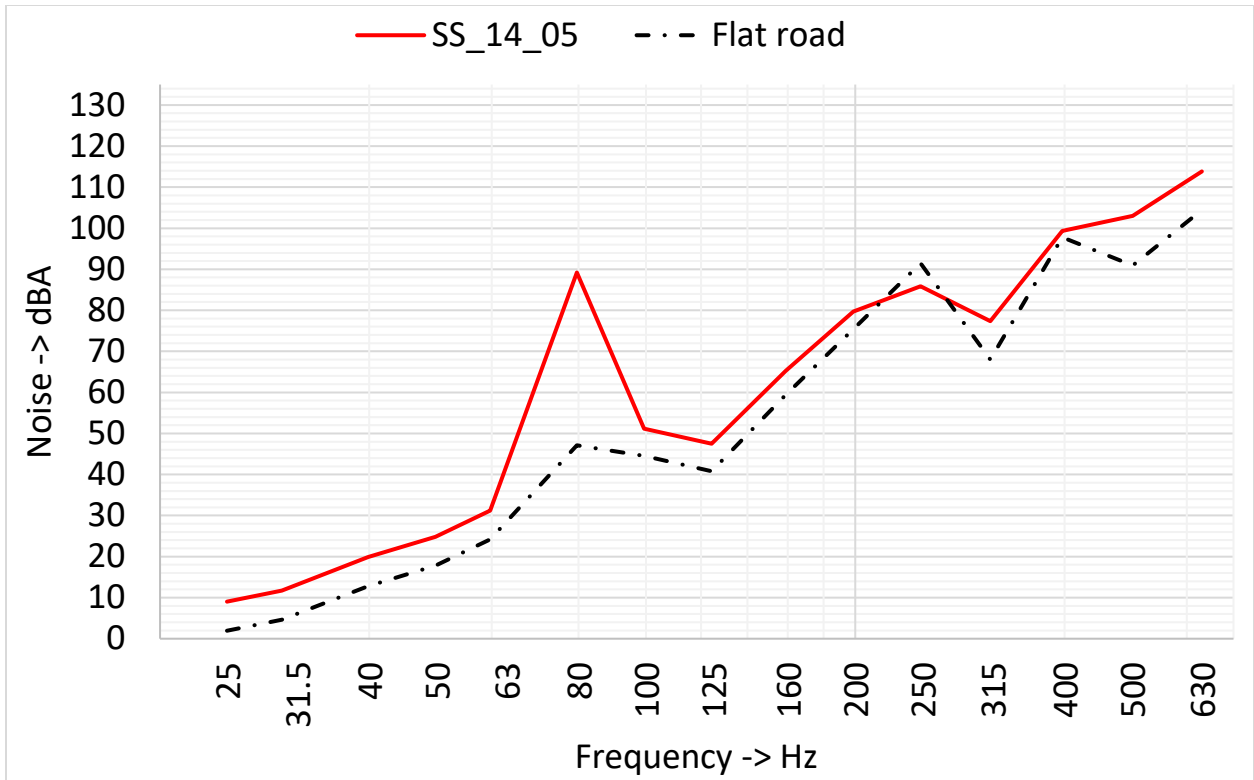


Figure A.7: 1/3 octave frequency spectrum for SS_14_05

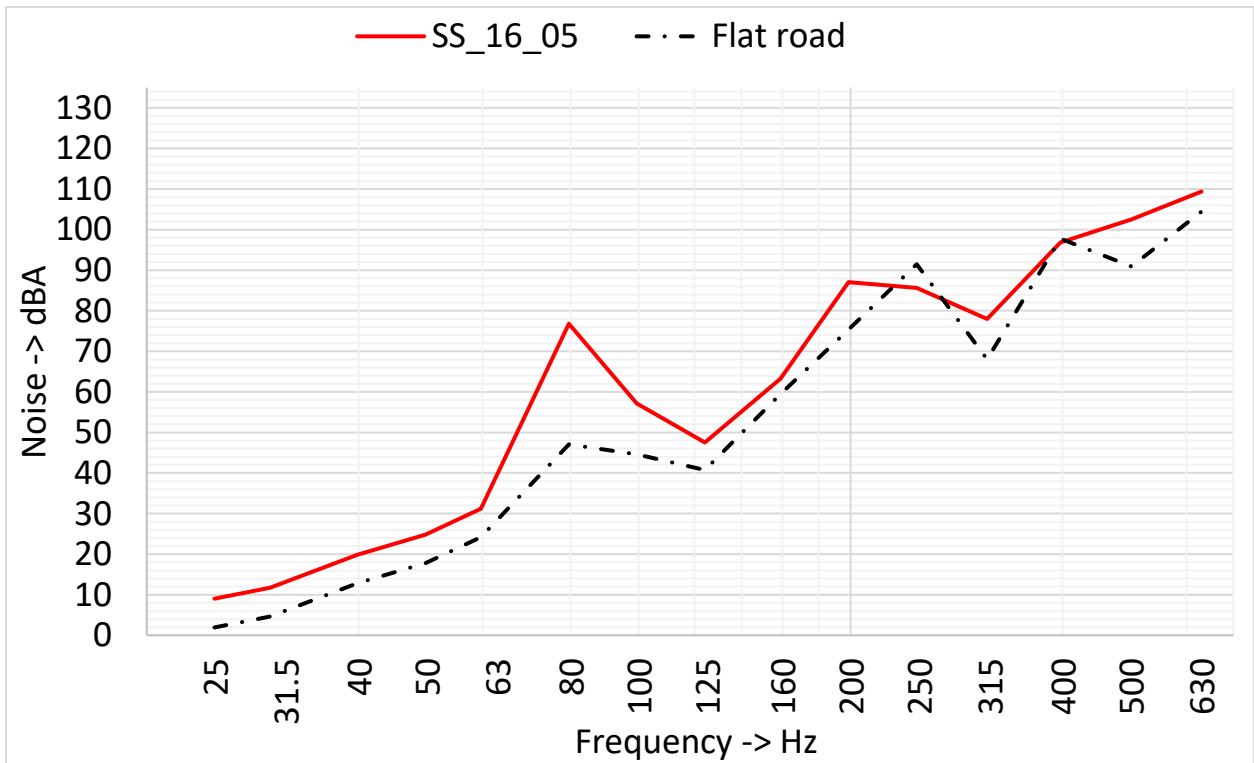


Figure A.8: 1/3 octave frequency spectrum for SS_16_05

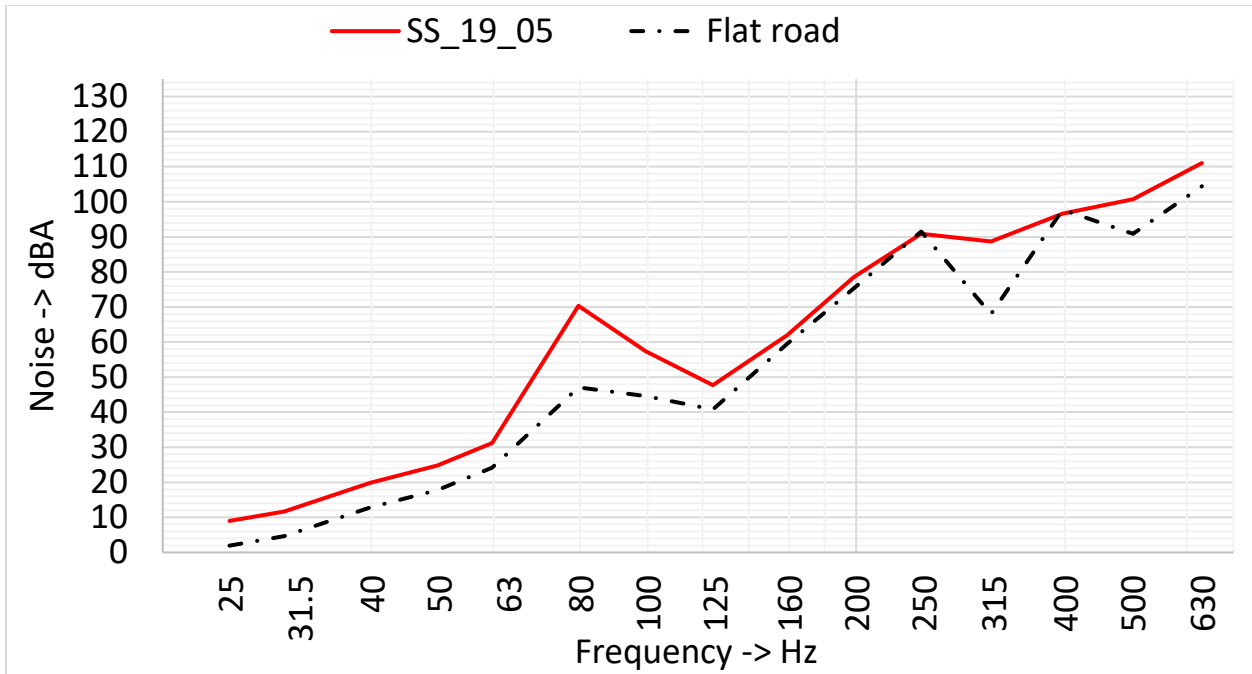


Figure A.9: 1/3 octave frequency spectrum for SS_19_05

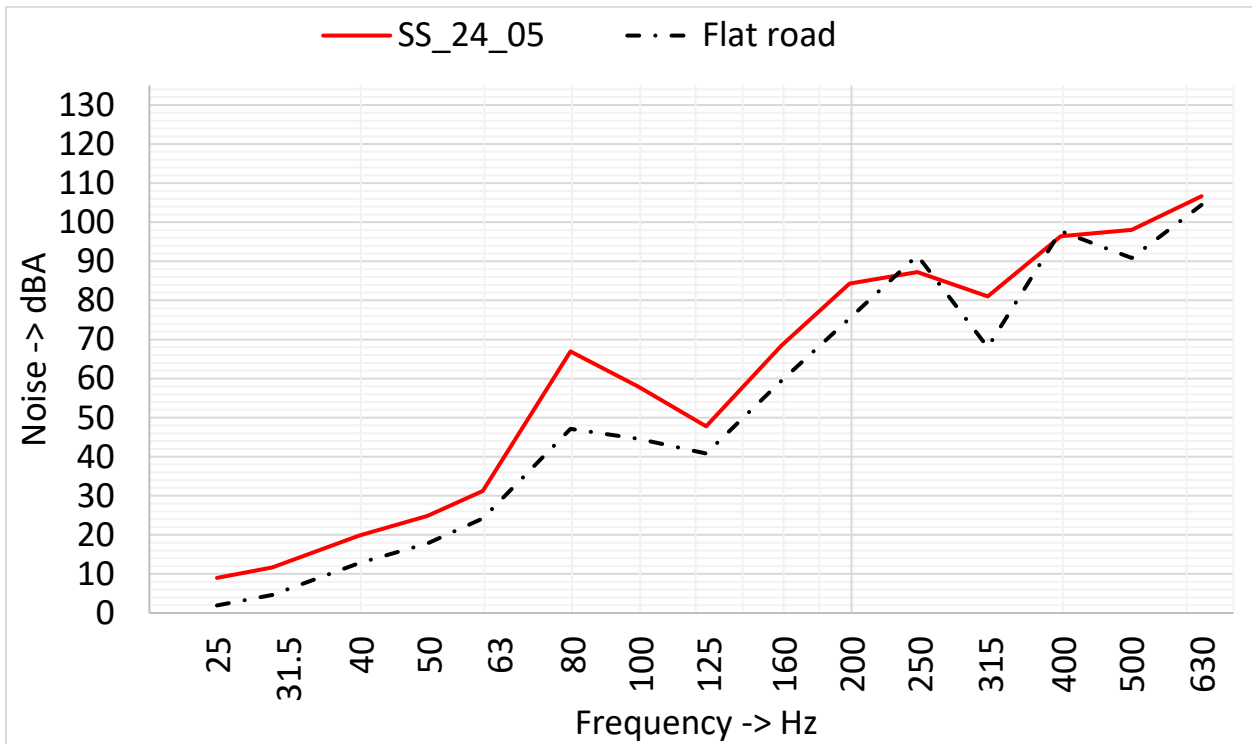


Figure A.10: 1/3 octave frequency spectrum for SS_24_05

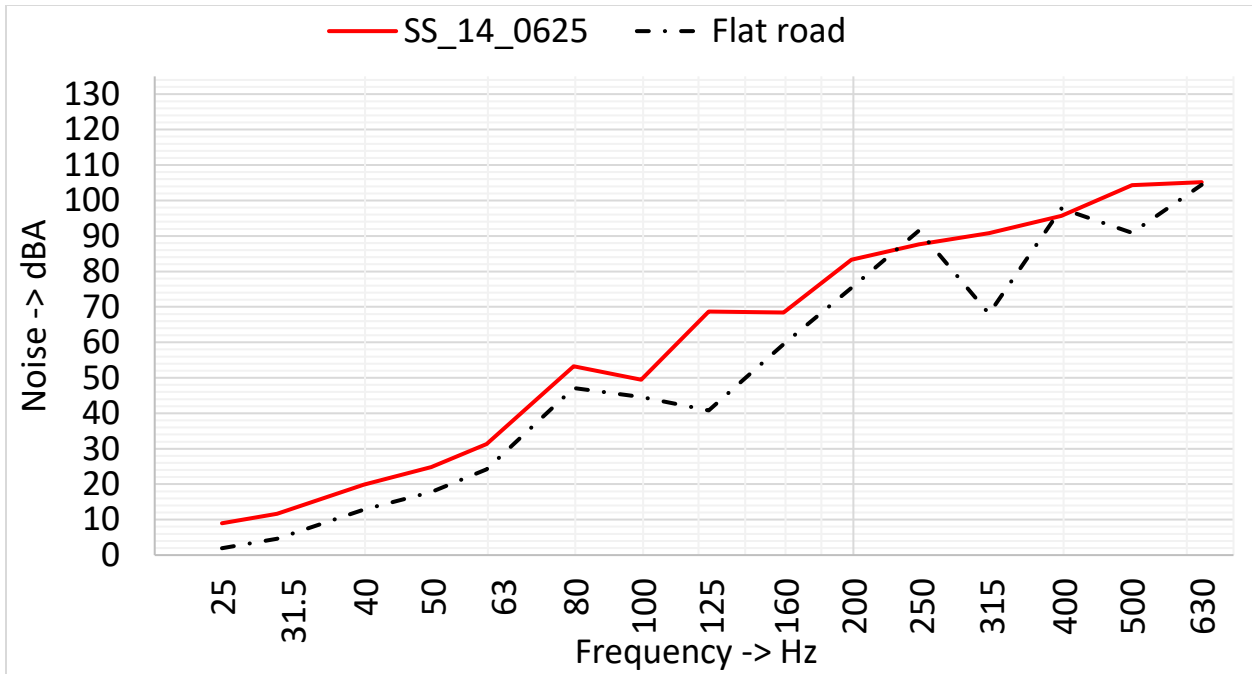


Figure A.11: 1/3 octave frequency spectrum for SS_14_0625

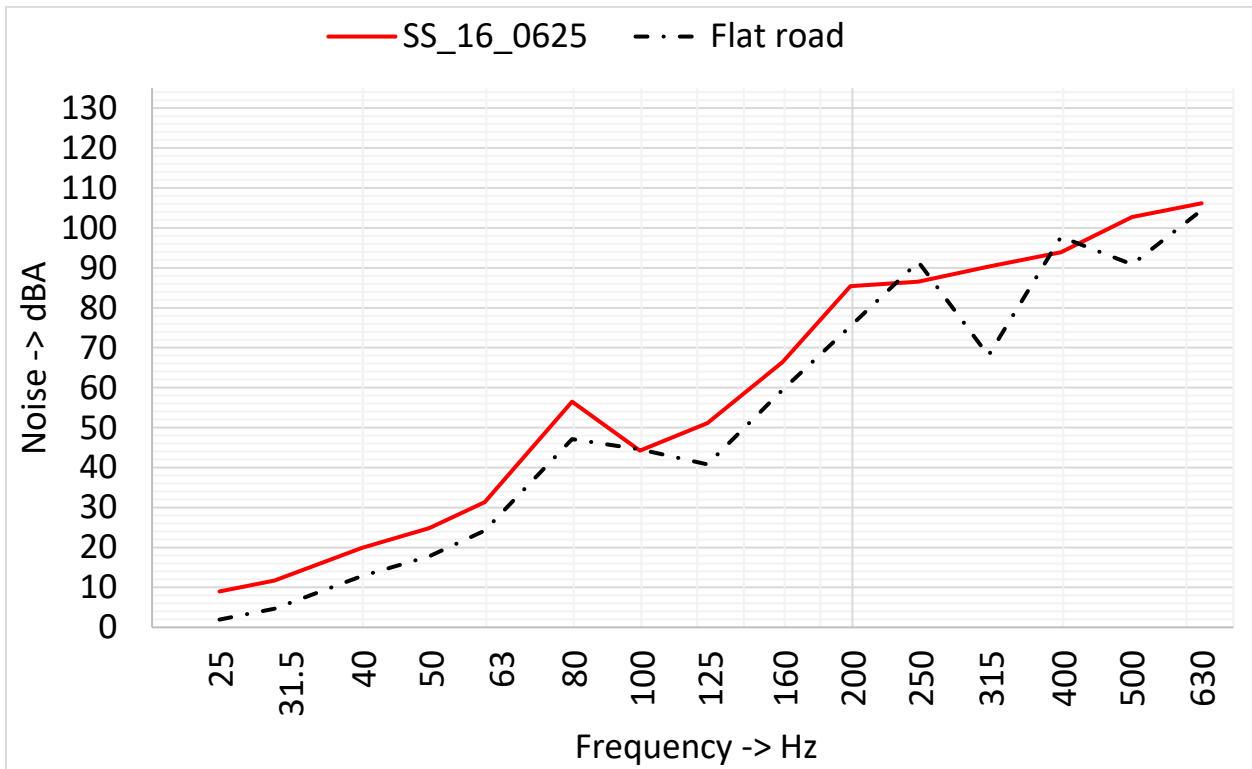


Figure A.12: 1/3 octave frequency spectrum for SS_16_0625

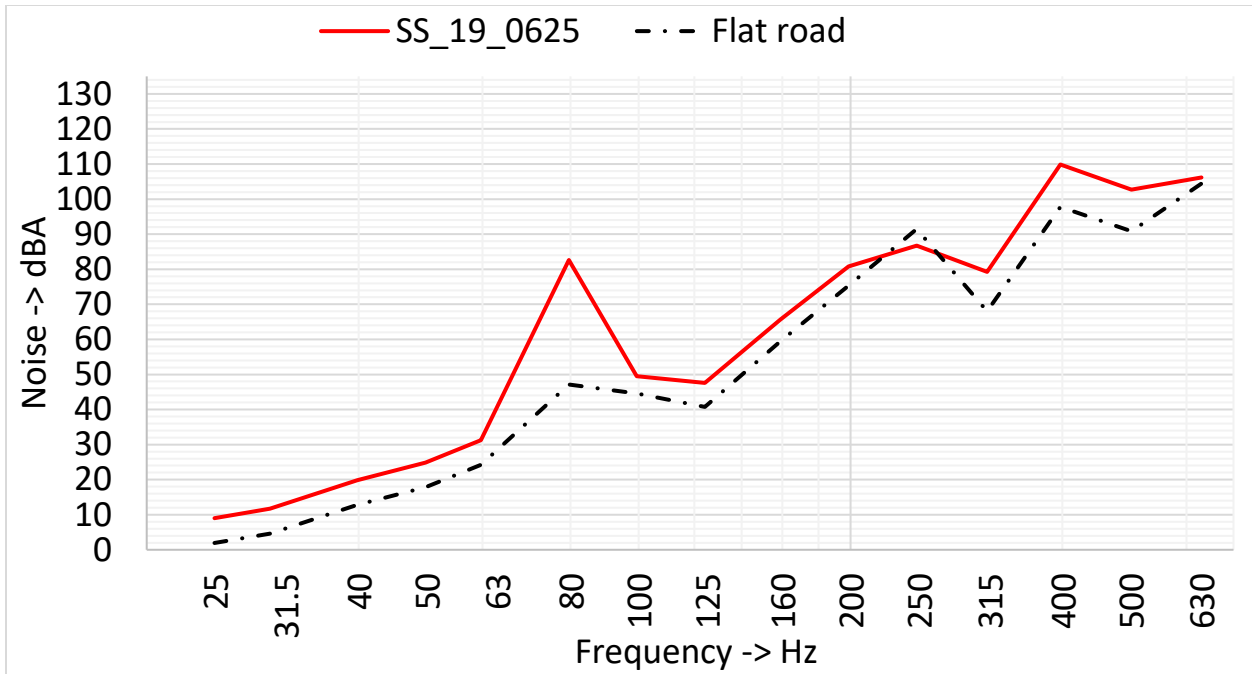


Figure A.13: 1/3 octave frequency spectrum for SS_19_0625

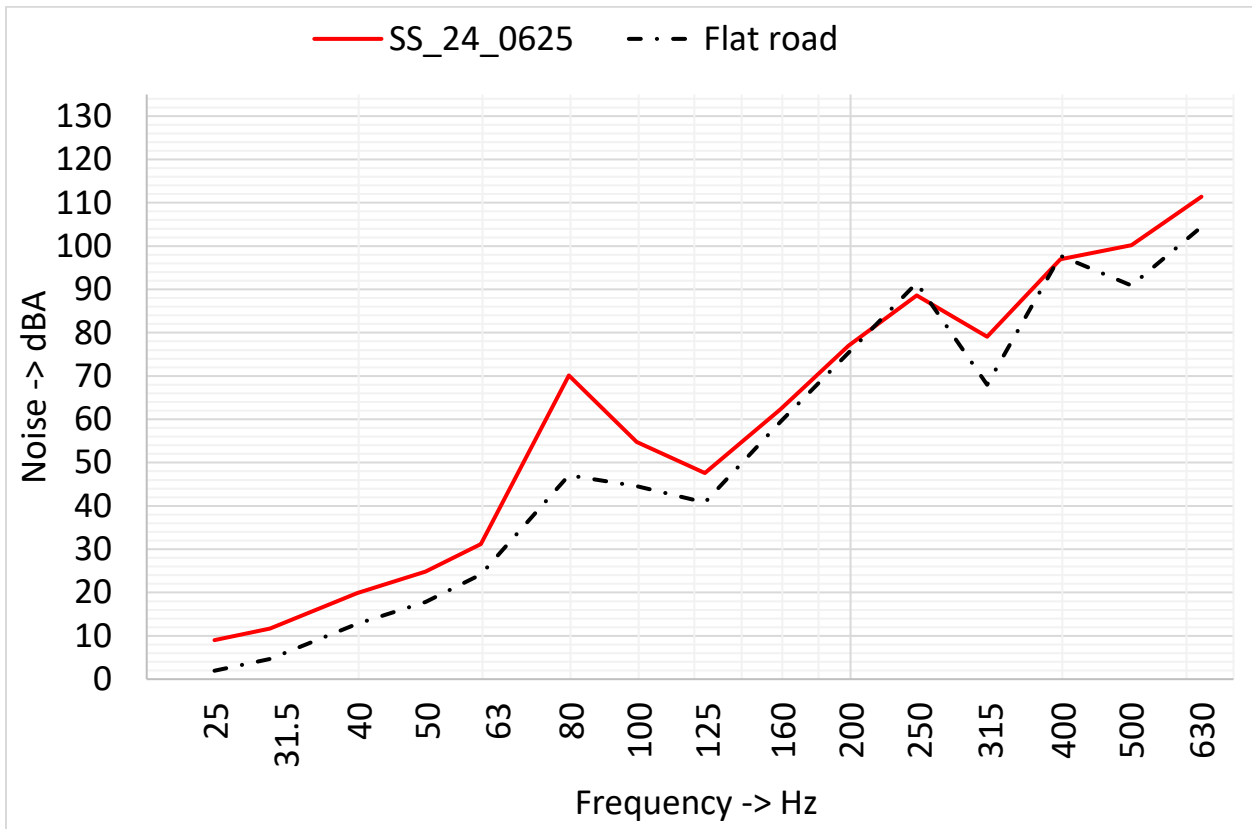


Figure A.14: 1/3 octave frequency spectrum for SS_24_0625

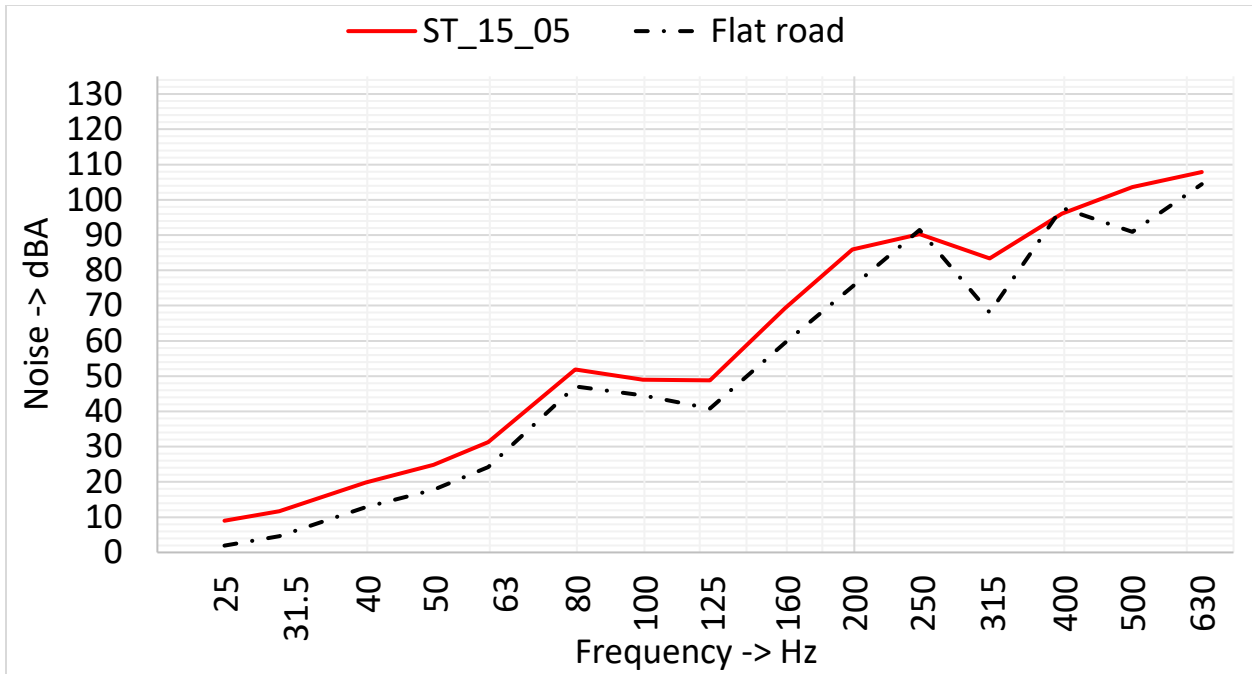


Figure A.15: 1/3 octave frequency spectrum for ST_15_05

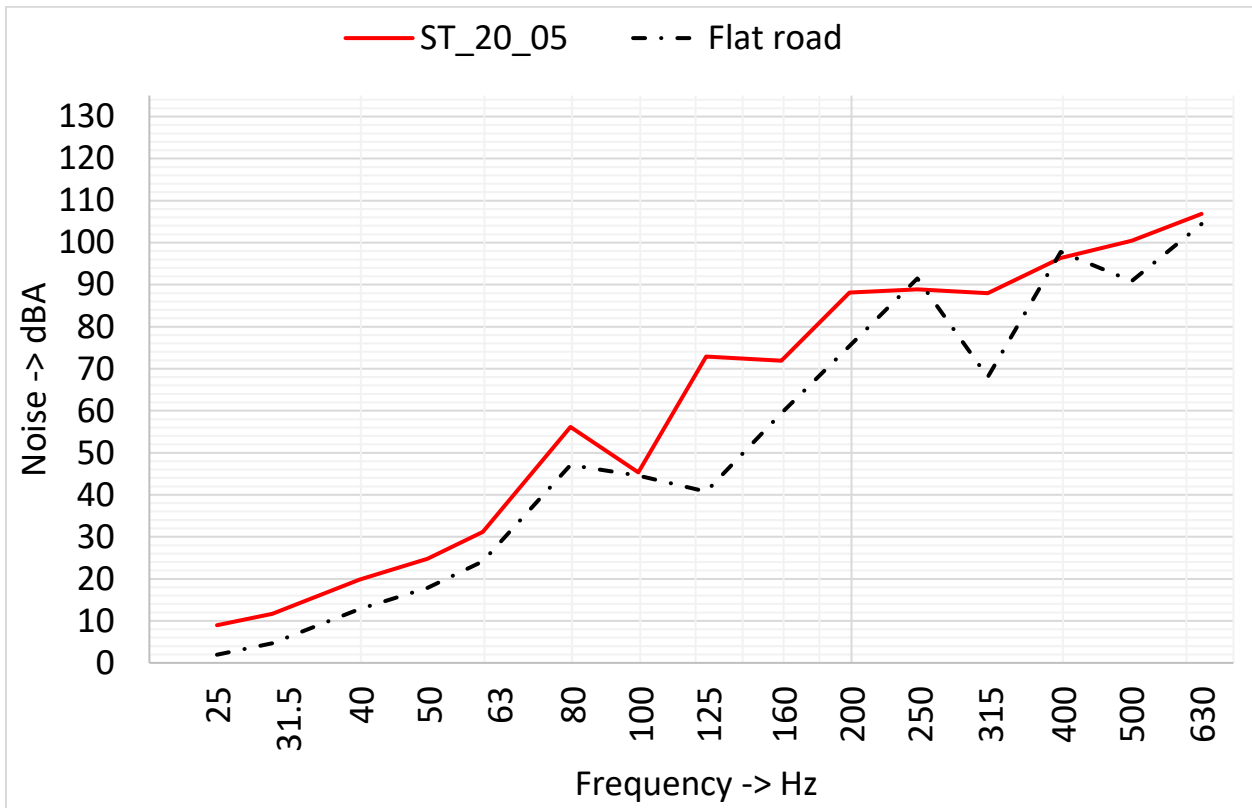


Figure A.16: 1/3 octave frequency spectrum for ST_20_05

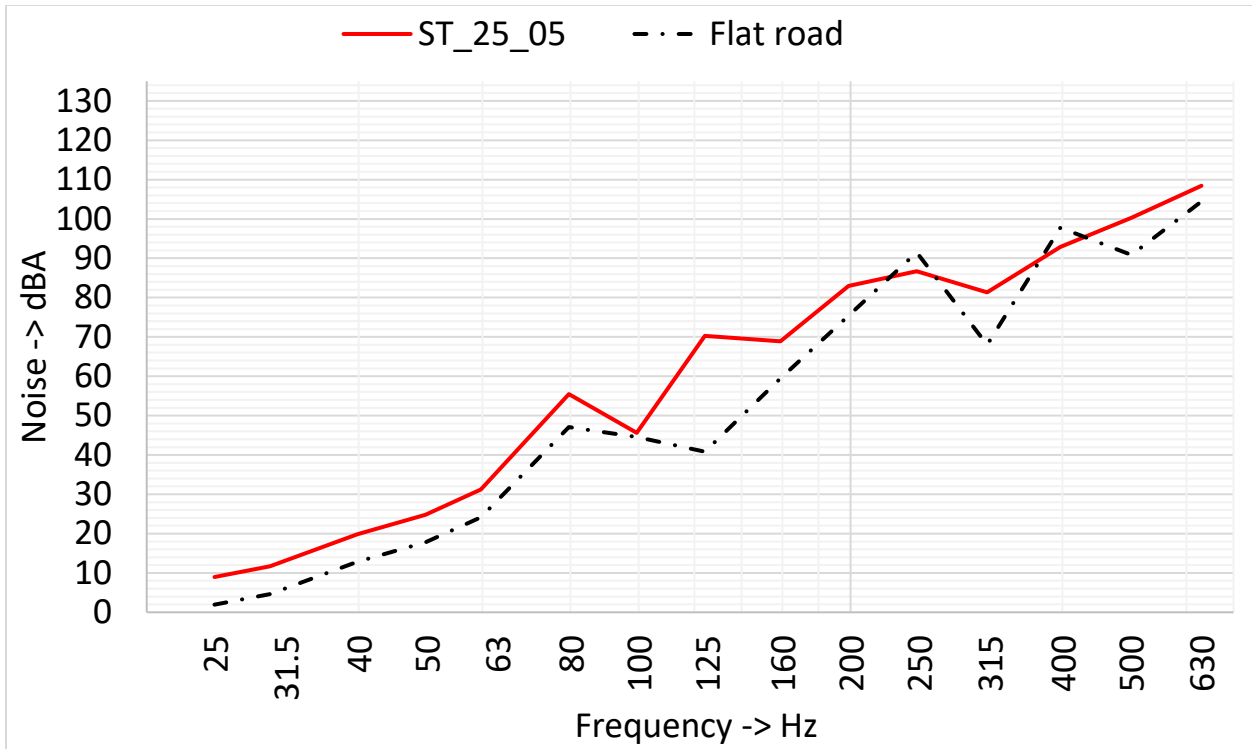


Figure A.17: 1/3 octave frequency spectrum for ST_25_05

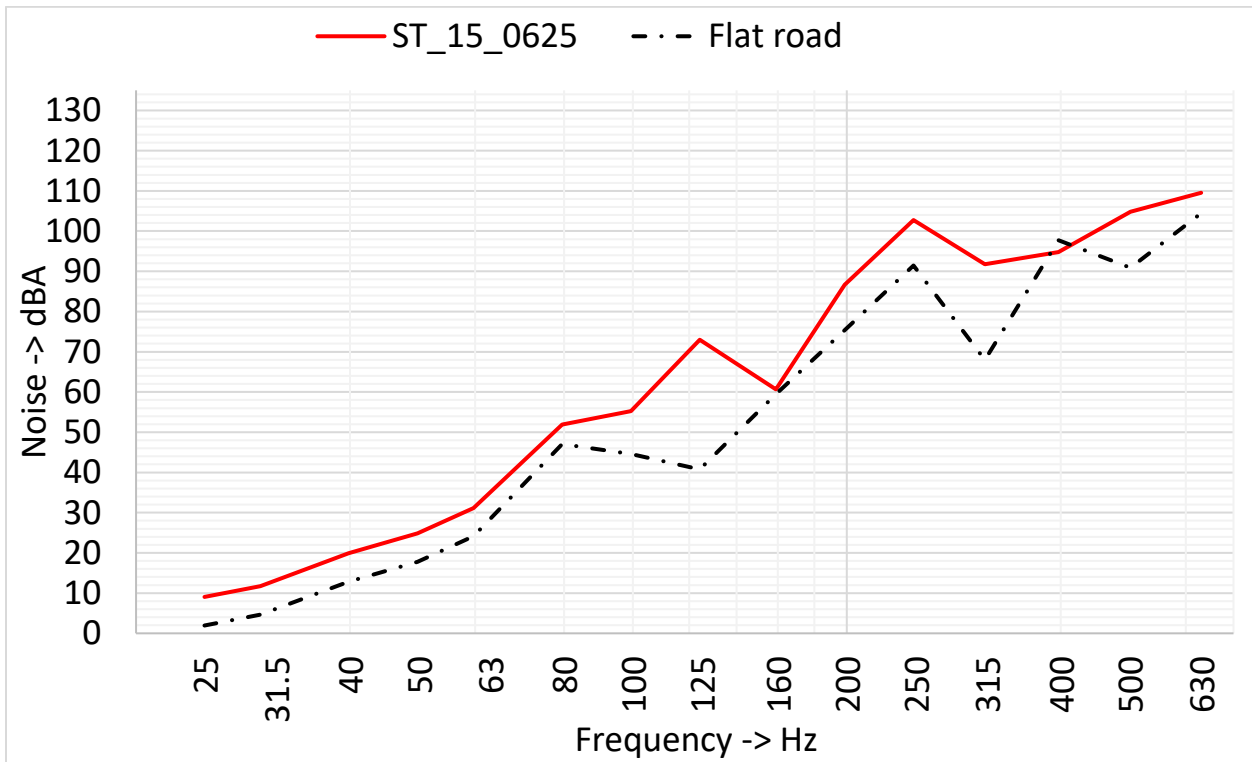


Figure A.18: 1/3 octave frequency spectrum for ST_15_0625

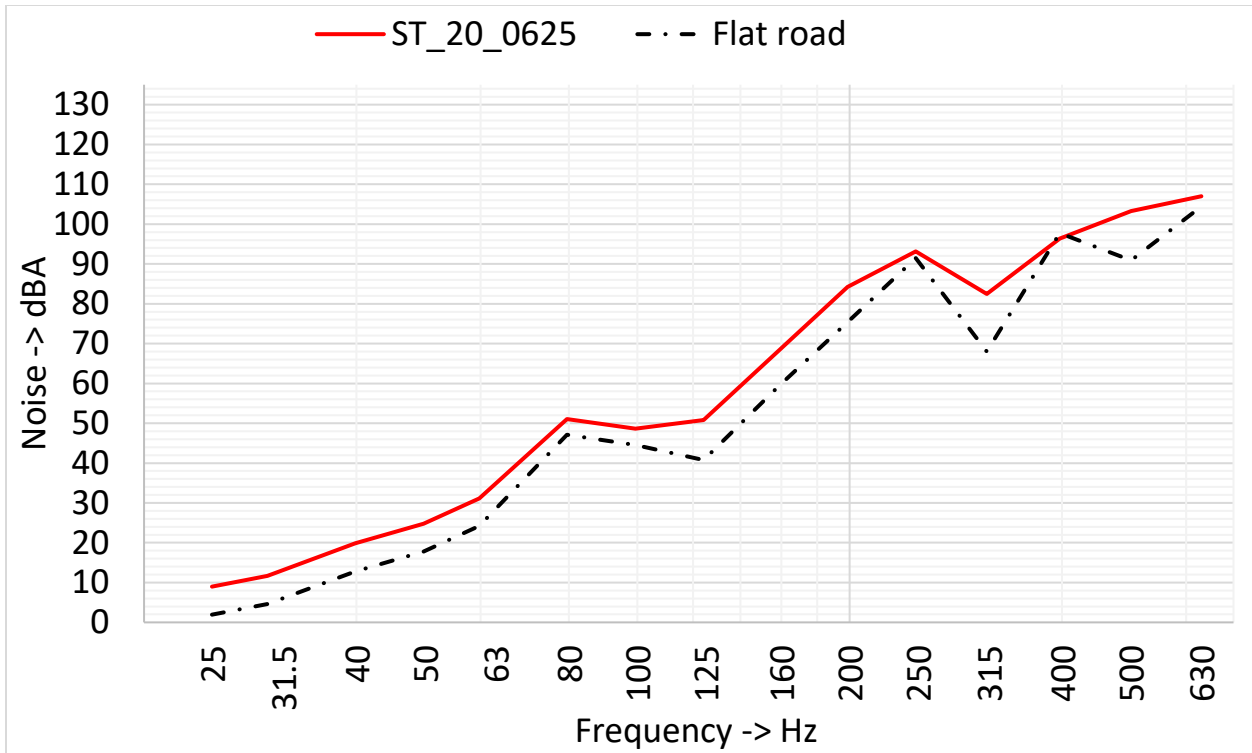


Figure A.19: 1/3 octave frequency spectrum for ST_20_0625

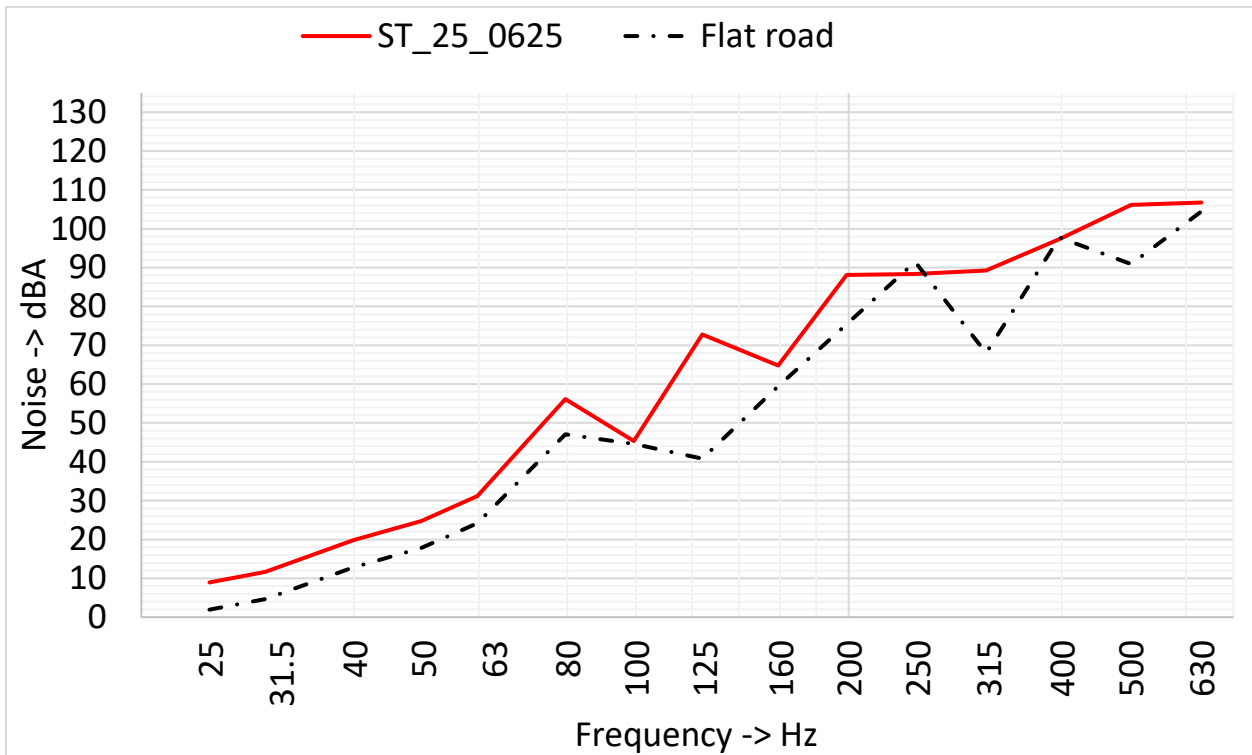


Figure A.20: 1/3 octave frequency spectrum for ST_25_0625